coatings

MDPI

Review

Nano–Bio Interface of Molybdenum Disulfide for Biological Applications

Rongrong Wu [1], Mingdong Dong [2] and Lei Liu [1,*]

[1] Institute for Advanced Materials, Jiangsu University, Zhenjiang 212013, China
[2] Interdisciplinary Nanoscience Center (iNANO), Aarhus University, C DK-8000 Aarhus, Denmark
* Correspondence: liul@ujs.edu.cn

Abstract: The unique nano–bio interfacial phenomena play a crucial role in the biosafety and bioapplications of nanomaterials. As a representative two-dimensional (2D) nanomaterial, molybdenum disulfide (MoS_2) has shown great potential in biological applications due to its low toxicity and fascinating physicochemical properties. This review aims to highlight the nano–bio interface of MoS_2 nanomaterials with the major biomolecules and the implications of their biosafety and novel bioapplications. First, the nano–bio interactions of MoS_2 with amino acids, peptides, proteins, lipid membranes, and nucleic acids, as well as the associated applications in protein detection, DNA sequencing, antimicrobial activities, and wound-healing are introduced. Furthermore, to facilitate broader biomedical applications, we extensively evaluated the toxicity of MoS_2 and discussed the strategies for functionalization through interactions among MoS_2 and the variety of macromolecules to enhance the biocompatibility. Overall, understanding the nano–bio interface interaction of two-dimensional nanomaterials is significant for understanding their biocompatibility and biosafety, and further provide guidance for better biological applications in the future.

Keywords: molybdenum disulfide; nano–bio interfacial interactions; biosensor detection; biological antibacterial; biocompatibility and biosafety

check for updates

Citation: Wu, R.; Dong, M.; Liu, L. Nano–Bio Interface of Molybdenum Disulfide for Biological Applications. *Coatings* **2023**, *13*, 1122. https://doi.org/10.3390/coatings13061122

Academic Editor: Seunghan Oh

Received: 24 May 2023
Revised: 13 June 2023
Accepted: 16 June 2023
Published: 18 June 2023

1. Introduction

Two-dimensional (2D) nanomaterials, such as graphene, hexagonal boron nitride (h-BN), phosphorene, and molybdenum disulfide (MoS_2) [1–3], have shown great potential in the field of biomedical applications. In particular, MoS_2, a representative transition-metal dichalcogenides (TMDs), has garnered substantial attention since its isolation in 2013 [4]. It is composed of a molybdenum (Mo) atom bonded with two sulfur (S) atoms in a layered structure, with the Mo and S atoms forming ionic bonds, and adjacent layers interacting with each other through van der Waals forces [5]. Notably, it can be easily separated into individual multilayers, with a single layer's thickness of 6.5 Å. The layered structure gives rise to their electronic properties with a tunable bandgap. Additionally, the distinctive mechanical and optical properties, as well as the high surface-to-volume ratio resulting from size reduction and planar surface morphology, contribute to their remarkable potential in a wide range of applications.

In particular, the crystal structure of MoS_2 is a fundamental factor that significantly influences its electronic, optical, and mechanical properties. Based on atomic stacking order, MoS_2 exhibits different crystal phases, including 3R, 2H, 1T, and 1H [6]. Typically, natural MoS_2 is a mixture of hexagonal 2H–MoS_2 and rhombohedral 3R–MoS_2, and the unstable 3R-phase can transform into the stable 2H-phase upon heating. Different polytypes may exhibit variations in their band structure, electronic states, optical absorption and emission properties, structural stability, layer interaction, and interlayer forces. For example, the 2H phase and 1T phase possess distinct electronic structures, where 2H-MoS_2 behaves as a semiconductor while 1T–MoS_2 acts as a metal [7]. On the other hand, the synthesis

approaches employed for MoS_2 fabrication, such as chemical vapor deposition (CVD), physical vapor deposition (PVD), hydrothermal/solvothermal synthesis, mechanical exfoliation, or other techniques, play a critical role in determining the resulting crystal structure. The precise control of synthesis parameters enables the promotion of specific polytypes, tailoring the crystal structure of MoS_2 to achieve desired properties for diverse applications.

MoS_2 has wide applications in industrial fields, such as energy storage, catalysis, semiconductor devices, optoelectronics, and lubrication [8,9]. However, the emergence of nanoscale MoS_2 has led to advancements in biomedical fields. Remarkably, 2D, 1D, or 0D MoS_2 nanomaterials present unique opportunities for the development of innovative biomedical applications owing to their exceptional properties and biocompatibility [10]. Their integration into biosensing platforms enables the highly sensitive detection of biomolecules, while their utilization in bioimaging allows for the improved visualization of cellular structures and processes. For example, the MoS_2-based field-effect biosensor has been proposed for protein and DNA detection in the biosensor field, which is based on a direct semiconductor electrons band gap (1.8 eV) [11]. Additionally, MoS_2 has been used as a contrast agent in biological imaging applications, specifically for X-ray-computed tomography, due to the X-ray absorption properties of Mo [12]. Furthermore, the exceptional surface-to-volume ratio of 2D MoS_2 enhances its interaction with biological entities, facilitating targeted drug delivery and tissue engineering applications [13–15]. Moreover, it can also be used as an antibacterial and antifungal agent [16].

With these wide prospects of MoS_2 in biomedical applications, the interfacial molecular interactions of MoS_2 with various biomolecules have raised great concerns, which closely connect with the biocompatibility of these nanomaterials and the applications in the field of biomedicine [17,18]. First, in terms of the biosafety and biocompatibility of MoS_2, the expanding utilization of MoS_2 in vitro or in vivo both raise the possibility of human exposure to these nanomaterials in various ways. Recent studies have shown that when MoS_2 enters the human body, its biodistribution will be affected by forming protein coronas in the blood, and molybdenum is significantly enriched in liver sinusoid and splenic red pulp [19]. However, the long-term biotransformation of nanomaterials in vivo may also affect tissues and organs due to the interaction with biomolecules [20,21]. Therefore, predicting and circumventing nano–bio interactions can reduce the potential biotoxicity to some extent. On the other hand, these interactions also influence the adsorption, binding, and recognition of biomolecules on the surface of MoS_2, ultimately dictating the functionality and specificity of the nanomaterials. The effective utilization of nano–bio interactions can also promote the functional biomedical applications of MoS_2, such as targeted drug delivery, single-molecule protein sequencing, and antibacterial material design.

The interfacial interactions between MoS_2 and biomolecules are governed by various non-covalent forces, such as electrostatic interactions, van der Waals forces, hydrogen bonding, and hydrophobic interactions [22–24]. Although there have been some studies on the nano–bio interface of MoS_2 combined with existing experimental techniques and computational simulation methods, it is still relatively rare compared with its demand in biomedical applications. In this review, we focused on the recent findings on the interaction of MoS_2 with biomolecules and categorize these common fundamental biomolecules into amino acids, peptides, proteins, DNA, and phospholipids (Figure 1). Further, we reviewed the novel biomedical applications of MoS_2 based on the understanding of nano–bio interfacial interactions, including peptide and protein detection, DNA sequencing, and antibacterial therapy. On the other hand, these non-covalent interactions are closely related to the biosafety and biocompatibility of these nanomaterials; therefore, we summarized and evaluated the existing literature on the biosafety of MoS_2 nanomaterials, including the modification and functionalization of MoS_2 based on the nano–bio interaction to increase the biocompatibility and reduced toxicity. Finally, a concise overview of the current challenges and limitations encountered is presented. In general, gaining a better understanding of nano–bio interface effects is of significant importance for biocompatibility optimiza-

tion and promoting the utilization of 2D nanomaterials in biomedicine, biodetection, and biosensing applications.

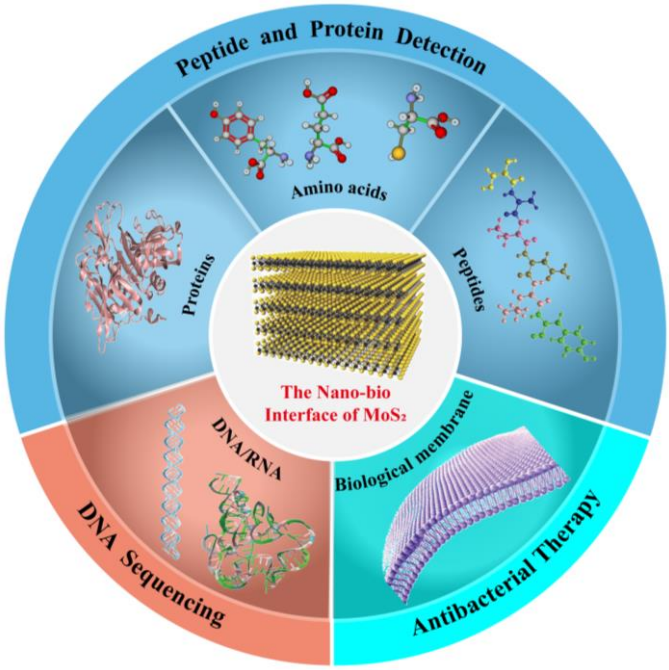

Figure 1. Illustrative representation of the different nano–bio interactions and their associated biological applications.

2. Interaction of MoS_2 with Various Biomolecules

In a sense, the nano–bio interaction between biomolecules and 2D nanomaterials is the essence of understanding the biocompatibility and biosafety of 2D materials. However, conventional experimental instruments face challenges in tracing the precise adsorption dynamics or conformation of biomolecules on the nano–bio interface. Density functional theory (DFT) and molecular dynamic simulation (MD) are both useful methods to obtain insight into the specific interaction mechanisms at the molecular level. These theoretical methods are widely used to explore biomolecular interaction and to evaluate nanoscale systems [25,26]. Herein, the detailed interactions between the major biomolecules and MoS_2 nanomaterials are summarized and followed by the applications based on these interactions.

2.1. Amino Acid Binding on MoS_2

Amino acids serve as the fundamental building blocks of proteins in animal nutrition, neurotransmitter transport, biosynthesis, and other vital functions [27,28]. The specific interactions between the standard 20 amino acids and the MoS_2 surface have recently been investigated [29]. Using density functional theory (DFT), researchers have systematically revealed the adsorption properties and electronic structures of amino acids on the surface of MoS_2. It is indicated that the adsorption strength of amino acids on MoS_2 surface follows a decreasing order: TRP > ARG > PHE > TYR > LYS > HIS > PRO > ASN ≈ MET > LEU > ILE > VAL > GLU > GLN > THR > ASP > CYS > SER > ALA > GLY (Figure 2A,B). The interaction between amino acids and the MoS_2 monolayer largely depends on the structural characteristics of the amino acids, with different side groups leading to distinct adsorption strengths. Amino acids possessing aromatic rings or long alkane chains exhibit higher adsorption capacity on the MoS_2 surface compared to other amino acids. Notably, a recent study also investigated the interaction between certain peptides (such as SER and CYS) and the MoS_2 nanopore using first-principles DFT calculations [30]. The study revealed that SER does not form any binding or interaction with the MoS_2 nanopore, yielding a

positive binding energy of 0.07 eV. Conversely, CYS can occupy the nanopore through non-bonding interactions.

In particular, the adsorption of amino acids on the MoS_2 surface has the potential to convert the chemical information into specific analytically measurable electronic and optical signals, for example, the construction of MoS_2-based field-effect transistors (FETs) using two representative amino acids of TRP and CYS [29]. The TRP/MoS_2 transistors exhibit a significant negative shift in the threshold voltage, from −25 V to −45 V, implying an enhanced electron injection from TRP to MoS_2. These biosensors primarily rely on the interaction between amino acids and MoS_2, allowing for precise detection and analysis. Consequently, the high sensitivity of the MoS_2 monolayer towards amino acids offers promising opportunities for the rational design and advancement of novel biosensors based on MoS_2.

2.2. Peptides and Proteins Mediated by MoS_2

Peptide is a kind of compound that is usually formed through dehydration and condensation reactions of 10–100 amino acids. They are important substances to synthesize cells or regulate various tissue functions of the human body [31]. For example, they can be used as neurotransmitters to transmit information and to transport various nutrients, vitamins, biotin, calcium, and trace elements to cells, organs, and tissues. As a potential biomedical material, MoS_2 nanomaterials have been paid close attention to and widely explored by researchers in the field of peptides interactions. For example, the abnormal aggregation of amyloid peptides in an aqueous solution will transform the soluble unstructured monomers into β-sheet rich oligomers and protofibrils, and finally become insoluble amyloid plaques, which are considered the main cause of Alzheimer's diseases (AD) and type-II diabetes [32–34]. Recently, MoS_2 has attracted much attention in regulating amyloid peptide fibrillization due to its specifical interfacial interaction between the 2D–MoS_2 surface and the amyloid peptides [35].

As mentioned above, the interaction between amino acids and MoS_2 strongly depends on the properties of the side chain of amino acids. Inevitably, the interaction between peptides or proteins and MoS_2 is also closely related to the amino acid composition. Previous studies have focused on the fundamental interaction by performing site-specific mutations on the peptide. For example, the native cecropin–melittin hybrid peptide adopts an alpha-helical secondary structure on the MoS_2 surface, with a non-parallel orientation that the hydrophobic C-terminus of the peptide readily interacts with MoS_2, while the hydrophilic N-terminal with more charged groups is not in contact with MoS_2 [36] (Figure 2C). The role of amino acids was verified by investigating the interaction between MoS_2 and three mutants of hybrid peptides, which indicated that the non-aromatic hydrophobic residues promote the interaction between the N-terminal and MoS_2. However, the presence of charged residues in the peptide hinders its direct contact with MoS_2 due to their tendency to interact with water. In another case, Zhou et al. [37] used the common antiparallel β-sheet structure model (YAP65 WW domain) to explore the effects of MoS_2 nanotube on the protein secondary structure modulation and the interaction between them. MoS_2 nanotubes cause considerable structural damage to YAP65 (Figure 2D). Essentially, the vdW interaction between YAP65 and MoS_2 nanotubes was the main force leading to adsorption (especially for aromatic residue, W39 and Y28), and glutamines such as Q26, Q35, and Q40 also made assignable contributions due to their long side chains and favorable interactions with MoS_2 nanotubes. More importantly, the adsorption of residues could be the main reason for the loss of the beta-sheet structure. Therefore, we can infer that of these amino acids, the hydrophobic residues with longer side chains are more likely to contact with MoS_2, while the conformation of peptide interactions with MoS_2 nanomaterials depends on the amino acid sequence. In addition, the cysteine that contains the thiol group has also attracted attention regarding its interaction with MoS_2 due to the S–S bond formation.

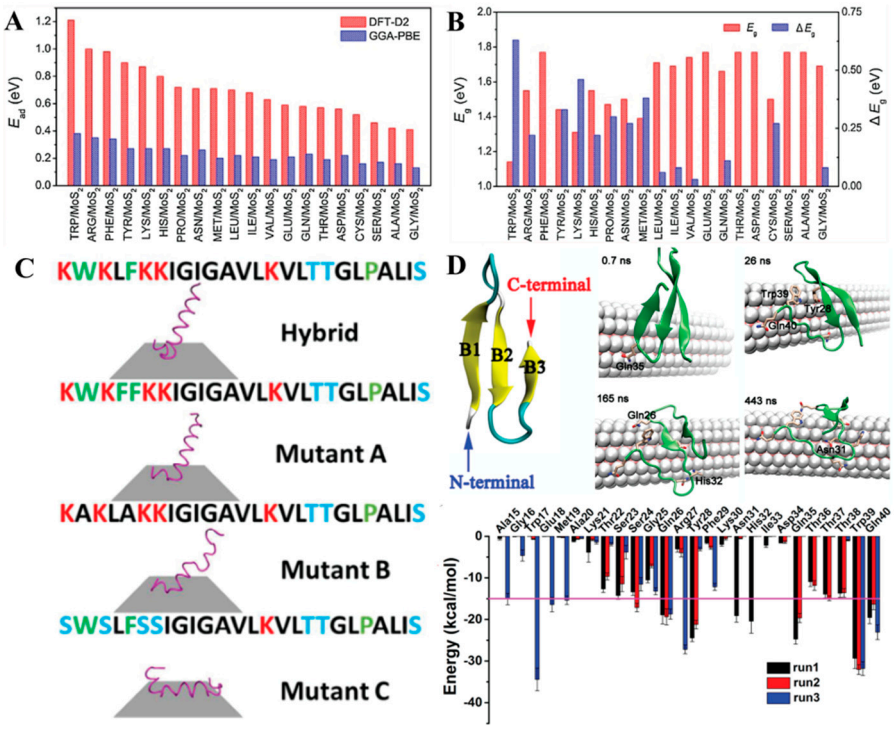

Figure 2. (**A**,**B**) Adsorption energy (E_{ad}) values of amino acid molecules on MoS_2 monolayer and the Energy gap (Eg) values of MoS_2 monolayer after the adsorption of amino acid molecules. Reprinted with permission from Ref. [29], copyright 2018 Elsevier. (**C**) Simulation results of cecropin–melittin hybrid peptide, mutant A, mutant B and mutant C on an MoS_2 surface. Reprinted with permission from Ref. [36], copyright 2018 RSC. (**D**) Snapshots of YAP65 interacting with MoS_2 nanotubes, and the interaction energy between them is shown. Reprinted with permission from Ref. [37], copyright 2016 ACS.

Based on the properties of these amino acids, proteins with hydrophobic contact surfaces will prefer to touch MoS_2 [38]. In particular, these adsorptions are often accompanied by protein denaturation, which usually involves the transient exposure of the hydrophobic protein core due to protein respiration and subsequent physical adsorption on the hydrophobic surface [39,40]. Different regions of protein contacting MoS_2 inevitably lead to different denaturation results. For instance, the lysozyme adsorption on the MoS_2 surface with six different orientations based on the different faces of lysozyme. Although the initial orientations of lysozyme were different, the adsorption orientation of lysozyme on the surface of MoS_2 tended to adopt the end-on orientation. It formed the "bottom-on" direction in orientations 1 and 5 (O1 and O5), while in O2, O3, O4, and O6 systems, it formed the "top end-on" orientation after reaching stable adsorption (Figure 3A,B) [41]. Among all those key residues, vdW interactions were found to be stronger than electrostatic interactions with the MoS_2 surface, including polar amino acids (N, G, S, G, T, Q), hydrophobic amino acids (L, W, P, A), and charge amino acids (R, D). Similarly, the effects of different binding modes of the $A\beta_{1\text{-}42}$ oligomer and the MoS_2 nanotube or nanosheet also prove this view [42]. The amyloid fibers were initially placed on top of the nanotube surface, with different β-sheets facing the nanotube (Figure 3C). In the orientation 1 (O1) system, all the chains interacted with the nanotube and were wrapped around the nanotube surface. However, in the system of orientation 2 (O2), the amino acids with a negative charge in the fibers oriented towards the MoS_2 nanotubes, the electrostatic repulsion resulting in the orientation changing and fiber contacting the nanotube at the edge, while in the systems of MoS_2 nanosheet, the fiber growth axis was perpendicular to the surface of MoS_2, and the stable composites were formed with only one chain contacting the nanosheet (Figure 3D). Therefore, the binding

mode and the nanostructure of MoS_2 have an obvious influence on the interaction between protein and MoS_2, especially for the orientation of the interface between them.

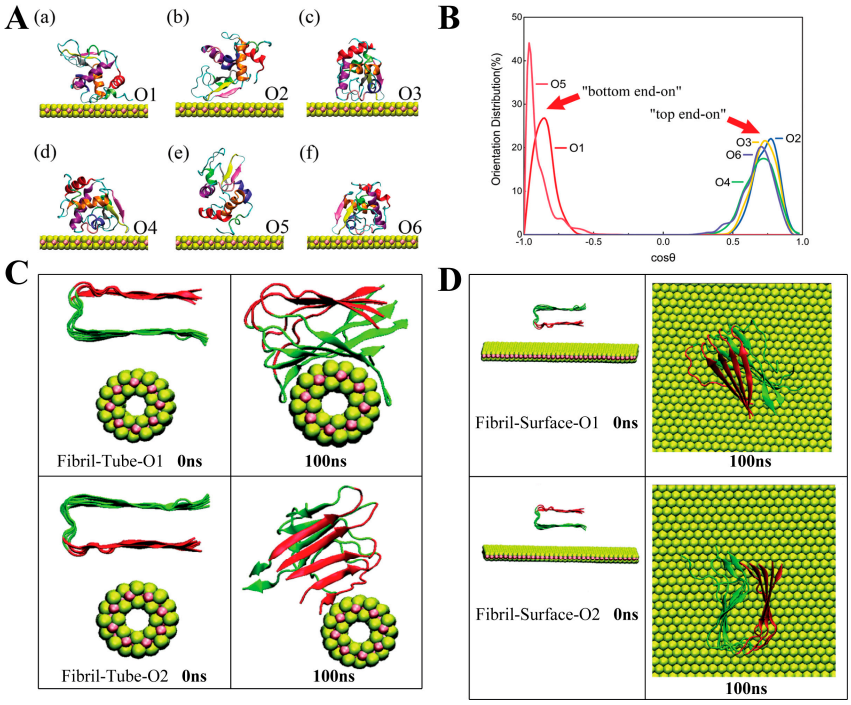

Figure 3. (**A**,**B**) Different orientations of lysozyme adsorbed on the MoS_2 surface. Reprinted with permission from Ref. [41], copyright 2017 Springer Nature. (**C**,**D**) The interaction between amyloid fibril and MoS_2 nanotube and nanosheet. Reprinted with permission from Ref. [42], copyright 2019 RSC.

The interactions between MoS_2 and proteins are closely related to the potential applications of MoS_2. Therefore, more exploration is sorely needed, especially for functional proteins. However, not all proteins could interact with MoS_2. For example, the interaction of MoS_2 with human serum albumin (HSA) and P53 protein has proven this statement (Figure 4A–C). MoS_2 preferred to interact with P53 rather than HSA [42]. The secondary structures of the two proteins were retained during the interaction process, with the drug-binding affinity of these proteins not being affected. Similarly, some current studies have shown that not all functional proteins could be affected by MoS_2. For example, Zhou and coworkers [43] have studied the interaction of MoS_2 with four ubiquitous potassium (K+) channels, including KcsA, Kir3.2, Kv1.2 paddle chimera, and K2P2 (TREK-1). These proteins are embedded in the plasma membrane to control the selective passage of potassium ions across the lipid bilayer and are ubiquitously distributed in different living cells. As shown in Figure 4D, for the KcsA channel, MoS_2 was able to significantly change the spatial arrangement of adjacent subunits and reshape the structure along the ion path. In the case of the Kir3.2 channel, the MoS_2 nanoflake was able to entirely cover the extracellular opening of the Kir3.2 channel, which probably blocks the normal K^+ ion conduction. As for the Kv1.2 chimera, MoS_2 is bound at the voltage sensor domain and intimately contacted with the N-terminal segment of S4. This binding would potentially influence the mobility of this important helix and might delay or disturb the normal gating process of the channel from the open to closed states. Similarly, the van der Waals force and the weak electrostatic force were the driving forces for this interaction process. Additionally, all of the hydrophobic, hydrophilic, aromatic, and charged amino acids play important roles in the interaction process. On the contrary, in the case of the K2P2/MoS_2 system, the large and rigid extracellular domain of K2P2 seemed to protect the channel from the interference of MoS_2 nanoflakes. MoS_2 was only bound to the extracellular top of K2P2, which did not change the overall or local structure of the channel. This may be since the large and rigid extracellular domain

of K2P2 is hydrophilic with negative charges distributed on the surface, which makes it difficult to combine with MoS_2. In addition, the interaction of MoS_2 nanoflakes with the ubiquitous mitochondrial porin voltage-dependent anion channel (VDAC1) was also explored [44], which is the most abundant protein in the outer membrane of all eukaryotic mitochondria. The MoS_2 nanosheet was able to insert into the lumen of the hVDAC1 hole to block it (Figure 4E). The initial contact was ascribed to the hydrophobic interaction between them, but subsequently, it was enhanced due to the complex hydrophobic and electrostatic interactions. Overall, the impact of MoS_2 on functional proteins can vary depending on the unique characteristics of each protein, leading to different interaction modes. The interactions between hydrophobic, hydrophilic, and charged amino acids in proteins and MoS_2 can affect the structural stability and functionality of proteins. Therefore, it is significant and pertinent to explore the influence of MoS_2 on peptides and proteins, on which lies the foundation for more beneficial applications in the future.

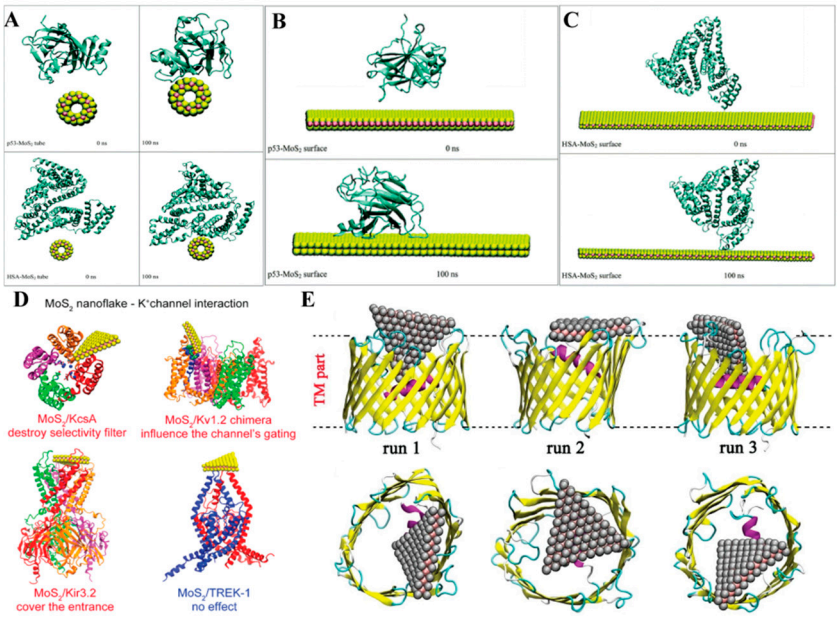

Figure 4. (**A**–**C**) Initial and final structures of p53 and HSA after interaction with MoS_2 tube and surface. Reprinted with permission from Ref. [42], copyright 2019 RSC. (**D**) Snapshots of the MoS_2 nanosheet interacting with K+ channels. Reprinted with permission from Ref. [43], copyright 2017 ACS. (**E**) Snapshots of the MoS_2 nanoflake binding to the hVDAC1 protein. Reprinted with permission from Ref. [44], copyright 2019 RSC.

2.3. Phospholipid Membrane Interacting with MoS_2

Among these current research works, the phospholipid is another group of biomolecules that is the main component of biological membranes, and it serves as the barrier to defend against attacking foreign agents and materials. Studying the interaction between 2D nanomaterials and lipid membranes will help us to better understand the mechanism of the antimicrobial activity or biosafety of these nanomaterials. Several mechanisms for the interactions of 2D nanomaterials with cell membranes have been proposed before (i.e., graphene oxide and MoS_2), including chemical oxidation and physical disruption [45,46], chemical oxidation can take place either through the formation of reactive oxygen species or via direct electron transfer. Physical damage may be initiated through the direct contact of 2D nanomaterials with the lipid membrane, followed by the penetration of the cell membrane. The loss of membrane integrity may be transmitted via the pore formation, adsorption, or adhesion to the nano surface or the extraction of lipid molecules. Different kinds of nanomaterials may have distinct physical interactions with lipid membranes due to their various shapes, mechanical properties [47], and surface chemical properties of nanomaterials [48]. Zucker and coworkers [49] have shown that graphene oxide (GO),

reduced graphene oxide (rGO), and MoS_2 nanosheets can mediate the lipid membrane disruption, while copper oxide (CuO) and iron oxide nanomaterials reverse it. Therefore, it is suggested that the shape and morphology are not sufficient to cause the loss of membrane integrity, and more complicated factors should be considered.

In theory, Zhou et al. reported the interactions between carbon-based nanomaterials (graphene and GO) and bacterial lipid membranes through MD simulations [50]. Graphene and GO exhibit strong interactions with phospholipid molecules and can insert themselves into the phospholipid membrane due to their hydrophobicity and the van der Waals force between them. Simultaneously, phospholipid molecules adhere to the surface of graphene and GO, leading to rapid damage to the stable lipid membrane structure (Figure 5A); compared to graphene, MoS_2 exhibits similar hydrophobic properties but has a thicker structure and a negative surface, resulting in different behaviors during the interaction with phospholipids [51] (Figure 5B). The MoS_2 nanosheets come into close contact with the lipid membrane due to their hydrophobic natures. Subsequently, the formation of depressions on the lipid membrane is co-dominated by van der Waals forces and electrostatic forces between MoS_2 and the membrane. Moreover, the electrostatic force derived from the surface charge characteristics of MoS_2 plays a significant role in extracting phospholipid molecules from the membrane.

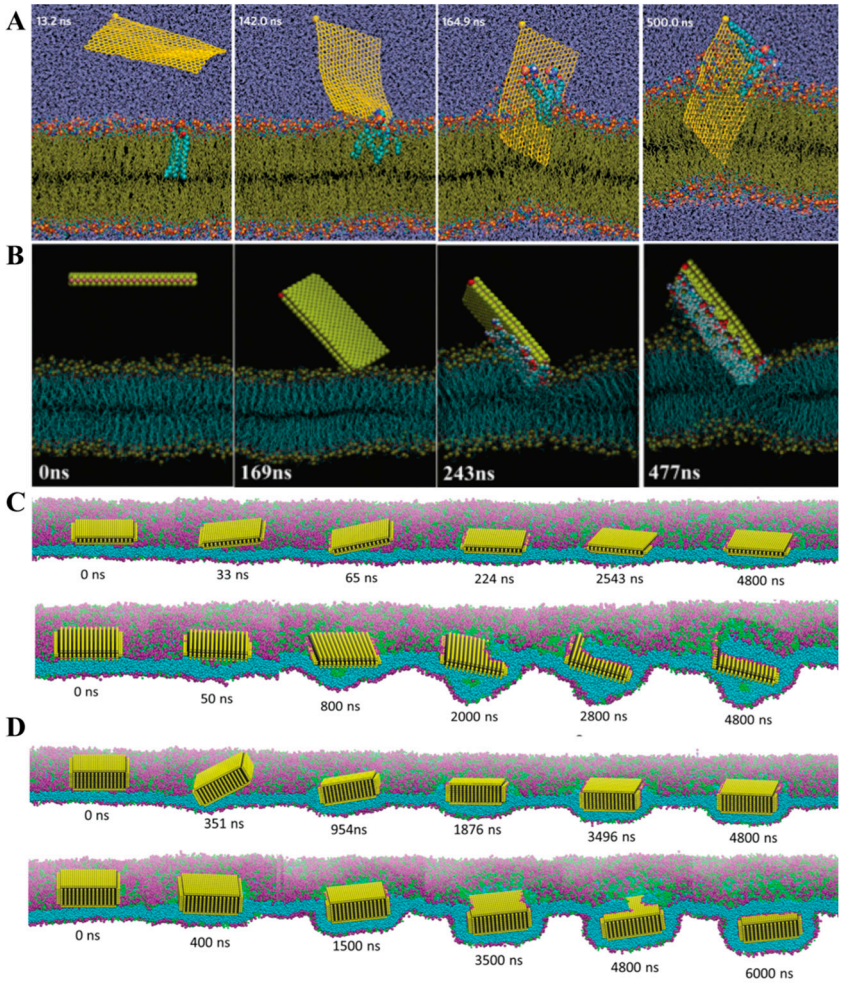

Figure 5. (**A**) Snapshot of graphene nanosheet interaction with phospholipid membrane. Reprinted with permission from Ref. [50], copyright 2013 Springer Nature. (**B**) Snapshot of MoS_2 nanosheet interaction with phospholipid membrane. Reprinted with permission from Ref. [51], copyright 2018 RSC. (**C**,**D**) Few-layered (**C**) and multilayered MoS_2 nanosheets (**D**) binding on the plasma membrane surface. Reprinted with permission from Ref. [52], copyright 2019 ACS.

Furthermore, different physical forms of MoS_2 nanosheets exhibited distinct interaction phenomena on lipid membrane disruption. The 40-layer MoS_2 nanosheets were capable of being internalized by the lipid membrane, whereas the 5-layer MoS_2 nanosheets could only bind to the surface of the lipid membrane [52]. In the case of MoS_2 nanosheets with fewer layers, the lipid membrane attempted to wrap the nanosheet by tilting from the top surface; however, it ultimately settled at the membrane midplane without successful internalization. On the other hand, for the MoS_2 nanosheets with more layers, encapsulation was facilitated and completed through an endocytosis process when the membrane experienced low surface tension. Subsequently, the nanosheet's final position was below the center of the film, exhibiting a downward movement in the simulation (Figure 5C,D). In addition, phosphorene has also demonstrated its ability to disrupt lipid membranes and extract lipid molecules from the membrane, suggesting an interaction mechanism between lipids and phosphorene [53]. Therefore, the tendency of 2D nanomaterials to damage phospholipid membranes seems to be a common characteristic. On the other hand, researchers have observed distinct interfacial phenomena between graphene nanosheets and MoS_2. Graphene nanosheets can shear phospholipid membranes, lie flat within the lipid membrane, or adhere to the surfaces of the lipid membrane. This indicates the necessity for further research to determine the specific interactions between these 2D nanomaterials and phospholipid membranes, considering their distinct properties.

2.4. Nucleic Acids Interacting with MoS_2

The exploration of the interplay between 2D nanomaterials and DNA has emerged as a prominent and actively investigated domain in recent years. Understanding the underlying physical mechanism governing the interaction between DNA and monolayer MoS_2 is imperative for the comprehensive analysis of M_OS_2-based biosensors implemented in DNA detection and sequencing. Novel nanopore membranes composed of electrically active two-dimensional (2D) solid-state materials, including graphene and MoS_2, offer the capability to simultaneously measure the in-plane transverse electronic sheet current and ionic current [54,55]. For instance, Leburton and colleagues have previously demonstrated the capability of a graphene nanopore membrane to detect the conformational transition of a helical double-stranded DNA to a zipper DNA, in addition to accurately quantifying the number of nucleotides in a single-stranded DNA molecule [56]. Furthermore, they elucidated that the detection and precise localization of DNA methylation can be accomplished utilizing nanopore sensors fabricated from graphene or MoS_2 nanomaterials, facilitated by the application of external voltage biases (Figure 6A) [57]. It was proven that both single-stranded DNA (A20) and double-stranded DNA (AT20) exhibited quicker adsorption onto the graphene surface compared to MoS_2 (Figure 6B). MoS_2 exhibits potential advantages over graphene for methylation detection due to its weakened DNA–MoS_2 hydrophobic interaction, which can effectively mitigate the undesired adsorption of biomolecules on the MoS_2 substrate. Interestingly, a graphene–MoS_2 hetero-nanopore, wherein two nanosheets are stacked on top of each other, demonstrates the capability to facilitate the translocation of single-stranded DNA (ssDNA) through its central nanopore [58]. The ssDNA molecules with a random sequence staying on the MoS_2 side of the heterostructure would be quickly (within several nanoseconds) adsorbed on the graphene surface based on the van der Wall force between them (Figure 6 C,D). Notably, the stacking of nucleotides on the graphene surface predominantly occurs through strong π–π base interactions. Throughout the simulation trajectories, the nucleotides exhibit substantial interactions with the nanopore surface. These interactions arise due to the presence of positively charged Mo atoms in the exposed regions of the MoS_2 nanopores, facilitating non-specific interactions with the negatively charged phosphate groups ($PO4^-$) in the nucleotides. Moreover, the primary driving force enabling ssDNA passage through the heterostructure nanopore is the chemical potential difference between ssDNA on the graphene and MoS_2 surfaces. Consequently, this implies that the adjustment of the chemical potential difference can be a pivotal consideration when

selecting diverse combinations of new two-dimensional (2D) materials for the construction of suitable hetero-structural materials in future DNA sequencing applications.

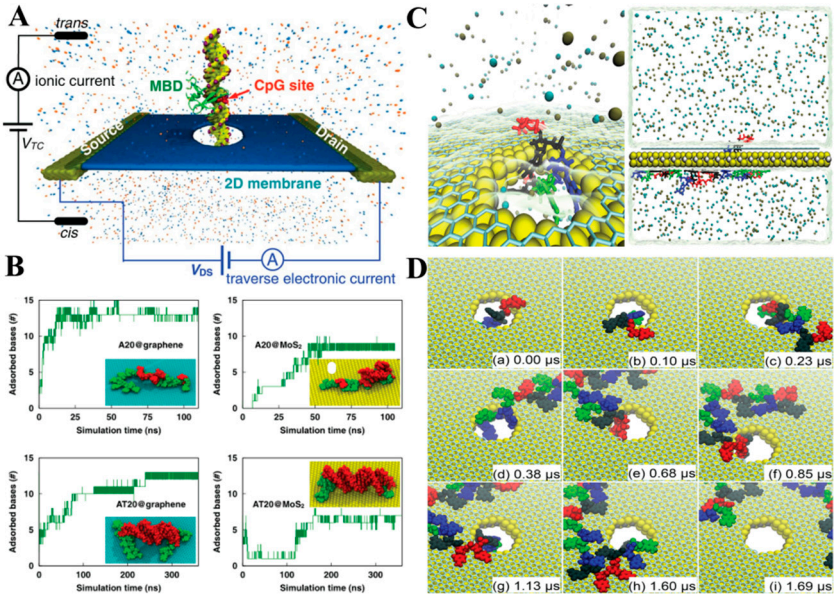

Figure 6. (**A**) Schematic of the nanopore device and (**B**) the comparison of adsorption capacity between graphene and MoS_2 surface. Reprinted with permission from Ref. [57], copyright 2017 Springer Nature. (**C**,**D**) MD simulation of ssDNA transport through graphene–MoS_2 heterostructure nanopore (**C**), and snapshots of a progressive transport (**D**) with the time evolution of the conformations (**a**–**i**) during the transport progress. Reprinted with permission from Ref. [58], copyright 2018 ACS.

3. Biomedical Applications Based on the Nano–Bio Interactions of MoS_2

MoS_2 characterized by its exceptional optical, electronic, and catalytic properties, as well as its remarkable capability for biomolecular interactions, has garnered significant attention within the scientific community. The investigation of intricate nano–bio interactions between diverse biomolecules and MoS_2 nanomaterials serves the purpose of broadening the scope of potential applications in the fields of biology and biomedicine, including drug therapy, biosensors, and antibacterial materials. Here, we mainly focus on elaborating the potential or recently attempted biological applications based on the interaction between MoS_2 and the biomolecules, peptide and protein, lipid membrane, and DNA, as mentioned above.

3.1. Peptide and Protein Detection

The simple, rapid, and sensitive detection of biomolecules is of great significance in clinical diagnosis, gene detection, and environmental monitoring. In recent years, MoS_2-based biosensors have demonstrated successful detection of a diverse range of analytes. When biomolecules are adsorbed onto the original MoS_2 surface, their chemical information, encompassing specific component details, can be effectively converted into analyzed electronic signals, and the band gap of MoS_2 can be significantly modulated [11,59]. Considering the pivotal role of amino acid sequences in protein folding and functionality, the ability to perform single-molecule protein sequencing holds great significance in identifying protein biomarkers and diagnosing various human diseases [60–62]. Although conventional protein sequencing methods exist, they still require improvements in resolution and sensitivity. Recently, Hayamizu et al. [63] reported that the monolayers spontaneously arranged non-covalently adsorbed peptides on the surface of MoS_2 transistors and used as biomolecular scaffolds for biosensing, as well as detected streptavidin. Moreover, Shen et al. [64] designed a $MoS_2/SnS_2/MoS_2$ hetero-structural platform, which can deliver an unfolded peptide to the nanopore-sensing region, depending on the different binding affinities of protein to two isomorphic materials.

Over the past few years, the nanopore analysis of 2D nanomaterials has emerged as a promising approach for single-molecule analysis, enabling the examination of unbroken protein chains and the detection of site-specific protein phosphorylation [65,66]. Notably, Kukkar et al. [67]. demonstrated a significant improvement in signal amplification for electrochemical protein-sensing by modifying gold screen-printed electrodes with MoS_2 nanoflakes, followed by conjugation with anti-BSA antibodies (Figure 7A). The electrochemical sensor platform displayed a linear response of peak current across varying concentrations of BSA up to 10 ng/mL, with an impressive minimum detection limit of 0.006 ng mL^{-1}. Similarly, the liquid-exfoliated MoS_2 nanosheet combing with carbon quantum dots (CDs) to detect cardiac troponin T (cTnT) [68] is an important biomarker for acute myocardial infarction. After cTnT interacted with anti-cTnT, followed by coating the surface of the CDs, the distance between MoS_2 and CDs increased and was followed by an increase in fluorescence intensity. Notably, the developed sensor is capable of reliably detecting concentrations as low as 0.12 ng mL^{-1}. The MoS_2 field-effect transistors (FETs) for detecting a prostate-specific antigen (PSA) can achieve sensitivity by adsorbing the anti-PSA onto MoS_2–FETs in a nonspecific way (Figure 7B). Additionally, it displayed a sensitivity and selective detection range from 1 pg mL^{-1} to 10 ng/mL [69]. Consequently, this innovative methodology holds great potential for enhancing the sensitivity and selectivity of protein detection methodologies.

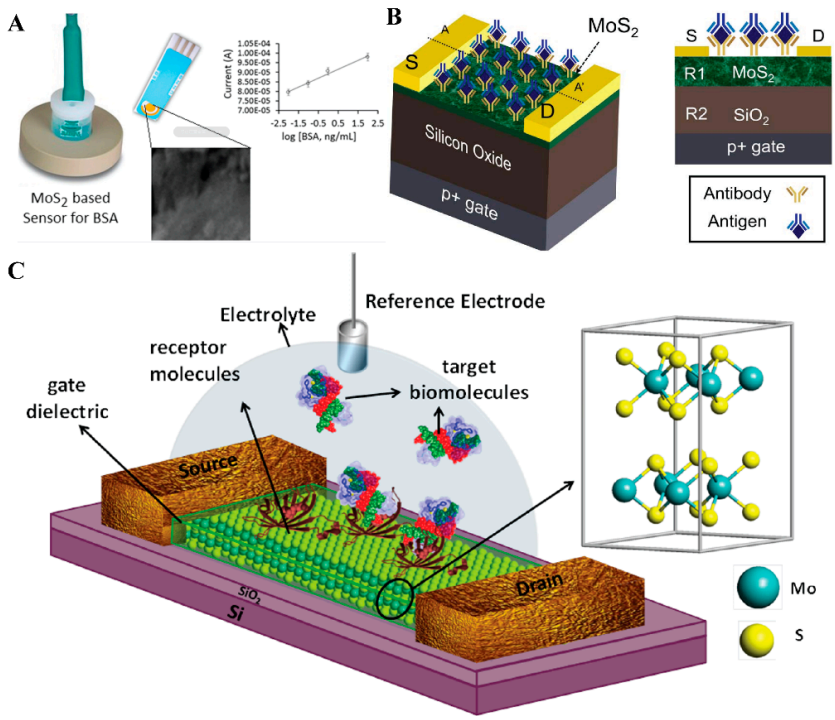

Figure 7. (**A**) Detection of MoS_2–based sensor for BSA. Reprinted with permission from Ref. [67], copyright 2016 Elsevier. (**B**) Schematic of the device used for numerical simulation. Reprinted with permission from Ref. [69], copyright 2017 Springer Nature. (**C**) Schematic diagram of MoS_2-based FET biosensor. Reprinted with permission from Ref. [60], copyright 2014 ACS.

In addition, Deblina Sarkar introduced and demonstrated the high sensitivity and easy fabrication of PH field-effect transistor biosensors using the 2D atomically layered MoS_2 materials (Figure 7C) [60]. Through theoretical analysis, they found that MoS_2 had a great benefit to the scaling of biosensor devices without affecting its sensitivity. The dielectric layer covers the MoS_2 channel, which is functionalized with receptors for specifically capturing the target biomolecules. When charged biomolecules are trapped, a gating effect is generated to regulate the device's current. Moreover, Sajid et al. developed a stable and high-efficiency impedimetric immunosensor capable of detecting multiple analytes by

using the electro-spraying of 2D MoS_2. The analytes included prostate-specific antigens, mouse immunoglobulin G, and the nuclear factor kappa-light-chain-enhancer of activated B cells [70]. Indeed, these findings underscore the remarkable potential of MoS_2 in the development of biosensors for protein detection applications.

3.2. DNA Detection and Sequencing

Nucleic acid detection, encompassing DNA and RNA analysis, holds paramount significance in various fields, including medical diagnosis, forensic medicine, cancer research, and environmental monitoring. The prevalent polymerase chain reaction (PCR) technology serves as a conventional DNA amplification and sequencing method in molecular diagnostics [71]. However, due to its high cost, pollution risk, and difficulty of use in diagnosis, it is necessary to develop a low-cost and highly sensitive detection method. MoS_2 exhibits size-dependent optical absorption, which is very important and valuable for the detection of DNA molecules.

In 2013, Zhang's group reported that a single-layer MoS_2 nanosheet can be used as an effective sensing platform for detecting DNA and small molecules, which is based on the ability of adsorption and fluorescence quenching for dye-labeled single-strand DNA (ssDNA) [72]. As shown in the schematic illustration (Figure 8A), an MoS_2 nanosheet is able to absorb the dye-labeled ssDNA through van der Waals forces between them, which could result in the quenching of fluorescence. However, when the ssDNA was probe-hybridized with its complementary target DNA to form a double-stranded DNA (dsDNA), the fluorescence intensity was recovered. The recovery of fluorescence is directly linked to the concentration of the target DNA in the system. Consequently, this feature has immense potential for accurately quantifying disease-related biomarkers in target DNA. Furthermore, a nanocomposite was developed based on the physical adsorption between MoS_2 nanosheets and conductive poly-xanthurenic acids [73]. The complementary DNA (cDNA) strands were incubated on the composite device to obstruct the electroactive surface area, thereby leading to an increase in the charge transfer resistance measured through electrochemical impedance spectroscopy. Following the introduction of tumor DNA, the hybridized double-stranded DNA isolated from the electrode surface facilitated the recovery of lower resistance in the conductance. Consequently, it can serve as a substrate for DNA immobilization, effectively reflecting the electrochemical transduction resulting from DNA immobilization and hybridization.

Based on the functionalized MoS_2 strategy, a thionin-functionalized MoS_2 electrochemical biosensor was further prepared [74], according to the intercalation and electrostatic interaction of thionin with DNA, the electrochemical response would be depleted, which can be used for detecting both dsDNA and ssDNA (Figure 8B). Yin's group [75] recently reported that the nanocomposite of MoS_2 and WS_2@PDA has the ability of DNA formation detection based on the photoactivity performance of this compound. The functional nanoprobe based on the MoS_2 nanosheet can also provide a smart, sensitive, and real-time intracellular miRNA detection platform. For example, DNA-functionalized layered TMDs have also attracted great interest for fabricating biosensors to detect miRNA-21 expression in cancer cell-based tumor microenvironments [76]. Mohamed Atef et al. [77] investigated the MoS_2 field effect transistor with a nanopore served for DNA base detection using the first-principle modeling. Both MoS_2 sheet and MoS_2 FET sensors exhibit distinct electronic characteristics for the different DNA nucleobases (Thymine, Adenine, Cytosine, and Guanine). Moreover, the dye-labeled ssDNA was absorbed on the MoS_2 nanosheet with fluorescence quenching. When the nanoprobe hybridized with the target miRNA inside the cancer cell (MCF-7 and Hela cells), it would result in the separation between MoS_2 nanosheet and dye-labeled ssDNA, leading to the recovery of green fluorescence (Figure 8C). Moreover, the block molecular beacons with poly-cytosine (polyC) tails anchored on MoS_2 nanosheets can also be used as probes for microRNA detection [78]. These polyC-mediated molecular beacons on MoS_2 possess very low background signal

and ultrahigh sensitivity, the specific detection of mononucleotide mismatches, and the selective detection of target microRNA in serum samples (Figure 8D).

Another application of DNA–MoS_2 biosensors is DNA sequencing. In particular, the utilization of single-layer MoS_2 with nanopores allows for DNA detection and sequencing. Nanopore-based DNA sequencing technology has the potential to enable the rapid and high-resolution identification of DNA bases. It has been reported that the suspended MoS_2 on silicon nitride (SiNx) film with a 20 nm thickness and controlled pore size could efficiently detect and sequence DNA [79]. Driven by the electric field of a pair of Ag/AgCl electrodes, DNA can translocate through the MoS_2 nanopore, and the ion current through the nanopore can be recorded by an axonpatch low-noise amplifier (Figure 8E). Moreover, Leburton et al. [80] developed a systematic algorithmic method to detect the presence of RNA tails on dsDNA using the single MoS_2 membrane nanopores as well as to identify the tail lengths from the transverse conductance signal. Liu's group [81] constructed a MoS_2/graphene heterostructure nanopores to test both dsDNA and native protein (BSA) at the single-molecule level in experiments. Through the different adsorption capacities of the two materials on biomolecules, the single-biomolecule translocation can be slowed and detailed information about biomolecules can be acquired. In general, the nanopore structure of 2D nanomaterials promotes the potential application of these materials in DNA sequencing with high selectivity and sensitivity. Therefore, it also verified the suitability and potential application for future bioanalysis and clinic diagnosis.

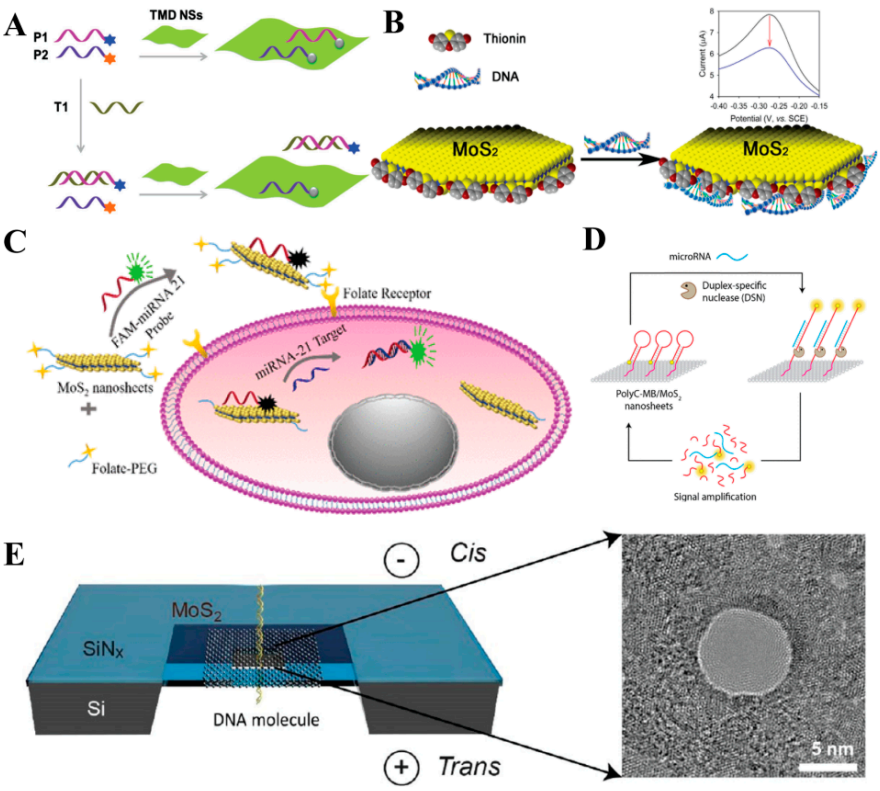

Figure 8. (**A**) Schematic illustration of single-layer TMD nanomaterial-based multiplexed fluorescent DNA detection. Reprinted with permission from Ref. [72], copyright 2015 Wiley. (**B**) Scheme of direct detection of DNA below the ppb level based on thionin-functionalized layered MoS_2 electrochemical sensors. Reprinted with permission from Ref. [74], copyright 2014 ACS. (**C**) Schematic of ssDNA–MoS_2–PEG–FA probe-based FRET platform for intracellular miRNA–21 detection. Reprinted with permission from Ref. [76], copyright 2017 ACS. (**D**) Schematic illustration of poly–C-mediated molecular beacons on MoS_2 nanosheets for microRNA detection. Reprinted with permission from Ref. [78], copyright 2018 ACS. (**E**) Schematic illustration of an MoS_2 nanopore membrane for DNA translocation. Reprinted with permission from Ref. [79], copyright 2014 ACS.

3.3. Antibacterial and Wound Therapy

The interaction between MoS_2 and the biological membrane is directly related to the integrality of cells, as well as the ecotoxicology and environmental impact of MoS_2 nanomaterial. Considering the inherent resistance of pathogenic bacteria to most commercially available antibiotics, the development of a new generation of antimicrobial materials with potent antimicrobial activity and low drug resistance has become a pressing and imperative task. As mentioned above, previous studies showed that 2D nanomaterials are very useful in this regard. In particular, MoS_2 has emerged as a highly promising candidate with significant antibacterial potential [45]. This potential stems primarily from the interplay between MoS_2 and the lipid membrane, as well as the synergistic effects of oxidative stress and the photothermal properties inherent to MoS_2. Liu's group and Roy's group explored the antimicrobial activity of MoS_2 nanosheets [82]; 60 μg mL^{-1} MoS_2 nanosheets were able to kill 96.6% of Gram-positive bacteria *S. aureus* or Gram-negative bacteria *E. coli* after 2h incubation. In the antimicrobial mechanism, the electrostatic interaction and strong van der Waal forces between lipid membrane and MoS_2 were revealed to cause the rapid depolarization of the membranes through dent formations, which resulted in drastic membrane disruption and the leakage of cytoplasmic contents. In addition, by inhibiting dehydrogenase enzymes and inducing metabolic stagnation in bacterial cells, it could lead to the inactivation of bacterial respiratory pathways. Moreover, the disruption of the membrane could induce the generation of oxidative stress, thus improving antimicrobial activity. It is further proven that MoS_2 could generate acellular/abiotic ROS. Therefore, the combination of ROS and oxidative stress induced by membrane damage could improve the overall efficacy of antimicrobial activity of the MoS_2 nanosheet (Figure 9A).

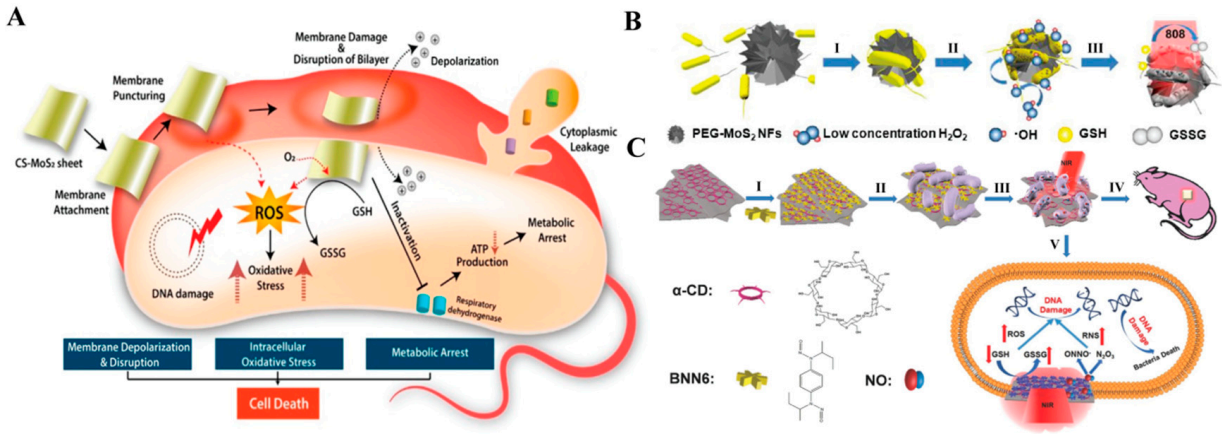

Figure 9. (**A**) Schematic illustration of the mechanism of antibacterial action of CS–MoS_2 nanosheets. Reprinted with permission from Ref. [82], copyright 2019 ACS. (**B**) PEG–MoS_2 as a combined system for the peroxidase catalyst–photothermal synergistic elimination of bacteria. (I) PEG–MoS_2 was captured by bacteria; (II) PEG–MoS_2 catalyze decomposition low concentrated H_2O_2 to generate ·OH to damage the cell walls integrity; (III) 808 nm laser irradiation causes hyperthermia, which accelerates GSH oxidation. Reprinted with permission from Ref. [83], copyright 2016 ACS. (**C**) Schematic illustration of MoS_2–BNN6 as a NIR laser-mediated NO-release nano-vehicle for synergistically eliminating bacteria. (I) α–CD modified MoS_2 (MoS_2–α–CD) assembly with BNN6 to form MoS_2–BNN6 through a simple hydrophobic interaction. (II) MoS_2–BNN6 was captured by bacteria. (III) 808 nm laser irradiation induced NO release improves bactericidal efficiency by synergetic PTT/NO. (IV) MoS_2–BNN6 used in wound disinfection and healing. (V) The antibacterial principle based on synergetic PTT/NO for elevating ROS/RNS while reducing GSH level. Reprinted with permission from Ref. [84], copyright 2018 Wiley.

Hyperthermia on MoS_2 surface under NIR irradiation also contributes to its antimicrobial activity. MoS_2 is often used as a photothermal transducer. Due to the high photothermal conversion efficiency, it induces bacterial cell death under NIR radiation. However, the

long-term irradiation of NIR laser with high power density will cause skin damage in photothermal therapy (PTT). Therefore, the combination of exogenous ROS and PTT will remedy the deficiency of a single modal antibacterial process, showing enhanced antibacterial activities in wounds. For instance, when the PEG–MoS_2 nanoflowers with high NIR absorption were combined with peroxidase, they were able to catalyze the decomposition of low concentration of H_2O_2 to generate -OH (Figure 9B) [83]. Such a reaction could show higher antimicrobial activity against the resistant bacteria, making the bacteria more vulnerable and more likely to heal. In order to give full play to the photothermal activity of MoS_2 against bacteria, the combination strategy was further developed. The functional MoS_2 nano-vehicle was able to mediate the release of nitric oxide (NO) via NIR irradiation, generating oxidative/nitrosative stress [84], which was able to kill the bacteria and facilitate the therapy of bacteria-infected wounds through combination with photothermal treatment (Figure 9C). Jaiswal et al. [85] developed a quaternary pullulan-functionalized 2D–MoS_2 glycosheets, which can be used as a potent bactericidal nanoplatform for efficient wound disinfection and healing, with the ability to synergistically destroys pathogenic strains and also helps in promoting wound-healing without causing any resistance generation. Its special antibacterial mechanism is based on a synergistic action of membrane damage and chemical oxidation or the distinct mechanisms of "pore-forming" and "non-pore-forming" pathways. In summary, in the disinfecting action of MoS_2, the interactions between MoS_2 and membrane play a leading role, which is the essence of the membrane disrupting mechanism and the ROS/PTT mechanism. The antimicrobial materials based on MoS_2 have a broad application prospects in future disinfection and wound therapy.

4. Biological Safety of MoS_2

The growing utilization of MoS_2 nanomaterials in biomedical applications has prompted substantial interest in studying their biological safety, particularly in the context of wound therapy and other in vivo applications. When these nanomaterials are introduced into the body through epidermal penetration or in vivo injection, the interactions with biomacromolecules become crucial determinants of their impacts on living organisms. Therefore, we finally reviewed the biological toxicity and safety of MoS_2 to develop more beneficial applications in vivo.

Multiple studies have consistently demonstrated the relatively low cytotoxicity of MoS_2 nanosheets across various in vitro cell lines. For example, Teo et al. [86] performed in vitro cytotoxicity studies involving three TMDs, including MoS_2, WS_2, and WSe_2. Their findings revealed that WSe_2 exhibited the highest toxicity, followed by MoS_2 and WS_2 nanosheets. Remarkably, both exfoliated MoS_2 and WS_2 showed significantly lower toxicity compared to graphene oxide. Therefore, MoS_2 possesses a broader range of potential applications. In another study, Fan et al. [87] investigated the cytotoxicity of multi-layered MoS_2 by using the NIH/3T3 immortalized dermal fibroblasts cell line. They observed a significant decrease in cell viability (~18%) with annealed MoS_2 sample, whereas the exfoliated MoS_2 samples exhibited no toxic effects. Additionally, Appel et al. [88] demonstrated that exposure to MoS_2 concentrations ranging from 0.1 to 100 μg mL^{-1} did not elicit any toxic effects, as evidenced by the absence of alterations in cell viability or intracellular ROS generation. Furthermore, studies on human cell lines, including CCC-ESF-1, A549, and K562, revealed that fullerene-like MoS_2 was non-toxic to cells [89].

In addition to the above in vitro cytotoxicity tests, the assessment of cellular uptake and inflammatory responses associated with MoS_2 nanomaterials provides further insights into their biological effects. These investigations have consistently shown that MoS_2 nanomaterials with a concentration of 1 μg mL^{-1} do not exhibit toxicity towards various cell lines, including A549 cells, AGS cells, and THP-1 cells. Notably, MoS_2 was observed to localize within single membrane vesicles, and the cellular morphology remained unaffected. However, it is worth noting that when administered at sub-lethal doses, the co-occurrence of endotoxin contamination may result in an inflammatory response [23]. Furthermore, some researchers [90] have demonstrated the effect of MoS_2 nanomaterials of different

sizes on the intestinal metabolome and microbiome in a mouse model. This revealed the ability to induce Mo accumulation into the small intestine and large intestine of mice after nano-MoS_2 and micro-MoS_2 enters the body through feeding. Importantly, both types of MoS_2 exposure changed the metabolic profiles of the intestine and intestinal microbiota, especially those involved in amino acid and carbohydrate metabolism. Notably, nano-MoS_2 exhibited a more pronounced pro-inflammatory effect compared to micro sized MoS_2. Hence, the aforementioned examples elucidate that the toxicity of MoS_2 nanomaterials is influenced by various factors, including size, thickness, and dosage administered in the body. Meanwhile, the biological effects vary across diverse cell and tissue models within complex biological systems, posing challenges for the in vivo application of such materials.

To reduce the cytotoxicity of MoS_2 and increase the dosage in vitro and in vivo, surface functionalization can be used to regulate the surface chemical and physical properties of MoS_2, etc. For example, polyethylene glycol functionalized (PEGylated) MoS_2 and WS_2 showed no appreciable acute toxicity to the treated mice at the tested dose (100 μg mL^{-1}) [91]. Additionally, it can be enriched in the reticuloendothelial systems (RES) for one month after intravenous injection, such as liver and spleen in vivo, and it would be completely excreted from the body by urine and feces within 30 d (Figure 10A) without apparent toxicity (Figure 10B). Wang and coworkers [92] also proposed that PEGylated MoS_2 showed no significant cytotoxicity after the 24 h-incubation of 4T1 cell, and the L929 cell models even at a concentration as high as 500 μg mL^{-1}. The surface PEGylation would also contribute to the enhanced cellular uptake of MoS_2 nanosheets [93]. Moreover, Chen et al. loaded poly (acrylic acid) (PAA) on the surface and further coupled it with PEG to form a hybrid nanosheet structure MoS_2–PPEG with better biocompatibility [94]. Therefore, the functionalized Mo-based nanomaterials with a variety of biocompatible polymers can improve the biosafety to some extent.

In particular, structural modification based on nano–biomolecular interactions has rarely been reported. For example, the chitosan-functionalized MoS_2 nanosheets have better biocompatibility and low cytotoxicity [12]. Moreover, the non-covalent modification of the MoS_2 surface with bovine serum albumin (BSA) has been recognized as an effective method to enhance the biocompatibility of MoS_2 nanosheets [95]. Recently, by combining them with the recognition function of nucleic acid aptamer (Apt), Shen et al. [96] constructed a composite material MoS_2–BSA–Apt, which possesses high photostability and photothermal effect, and good biological safety (Figure 10C). Importantly, it can target and identify tumor cells, and effectively ablate them through combination with laser irradiation. Moreover, Zhu et al. [97] synthesized bovine serum albumin-folic acid-modified MoS_2 sheets (MoS_2–PEI–BSA–FA), and combined the capping agent of block PMOs to control the drug release and to investigate their potential in near-infrared photothermal therapy. In particular, the drug-carrier complex (PMOs–DOX@MoS_2–PEI–BSA–FA) exhibited excellent photothermal transformation ability and biocompatibility in physiological conditions (Figure 10D). It possesses outstanding tumor killing efficiency and specificity to target tumor cells via an FA-receptor-mediated endocytosis process. Moreover, many other proteases can also be supported on the surface of MoS_2, such as sequence-based DNA oligonucleotides [98], α-chymotrypsin [99], RGD-targeting peptides [100], etc., thereby expanding the various biomedical applications of MoS_2 in vivo.

Moreover, the combination of MoS_2 with other nanomaterials can impart additional functionalities and synergistic effects, leading to enhanced bio-application outcomes. The incorporation of functional nanomaterials into MoS_2 nanocomposites can enable targeted drug delivery, improved imaging capabilities, enhanced tissue regeneration, and precise therapeutic interventions. For instance, the MoS_2/GO nanocomposites show favorable lung targeting and enhanced drug loading/tumor-killing efficacy with improved biocompatibility [101]. The form of nanocomposites not only expands the potential applications of MoS_2 in diverse biomedical fields but also contributes to its improved biosafety by promoting specific interactions with biological entities. To sum up, the biosafety and biocompatibility of MoS_2 nanomaterials are directly related to their intrinsic properties, which can be ad-

justed by modifying their structures, including changing the size and shape, biocompatible polymer functionalization, the surface loading of biomolecules, and the construction of nanocomposites (Figure 11). Investigating the biosafety of MoS_2 is vital for ensuring human health and safety, enabling the development of safe and effective biomedical applications, complying with regulatory requirements, managing risks associated with their use, and advancing the field of nanotechnology.

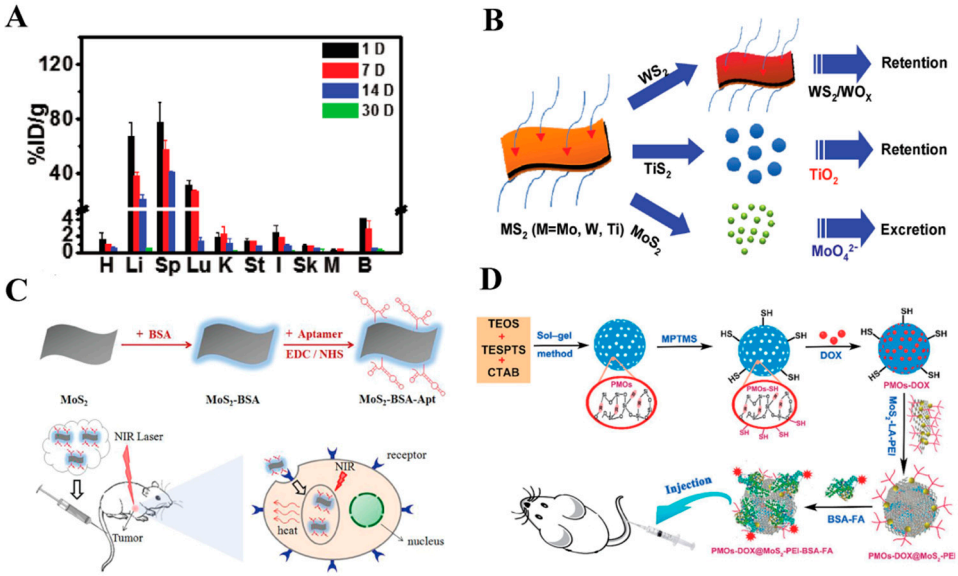

Figure 10. (**A**) In vivo bio-distribution of PEGylated MoS_2, and (**B**) the different pathways of the clearance of MoS_2–PEG nanosheets (M = Mo, W, and Ti). Reprinted with permission from Ref. [91], copyright 2016 Wiley. (**C**) Precise photothermal therapy of tumor-bearing mice with aptamer modified MoS_2 nanosheets. Reprinted with permission from Ref. [96], copyright 2021 Elsevier. (**D**) The synthesis and preparation of PMOs–DOX@MoS_2–LA–PEI–BSA–FA composite as a multifunctional drug-delivery system for tumor therapy. Reprinted with permission from Ref. [97], copyright 2018 Elsevier.

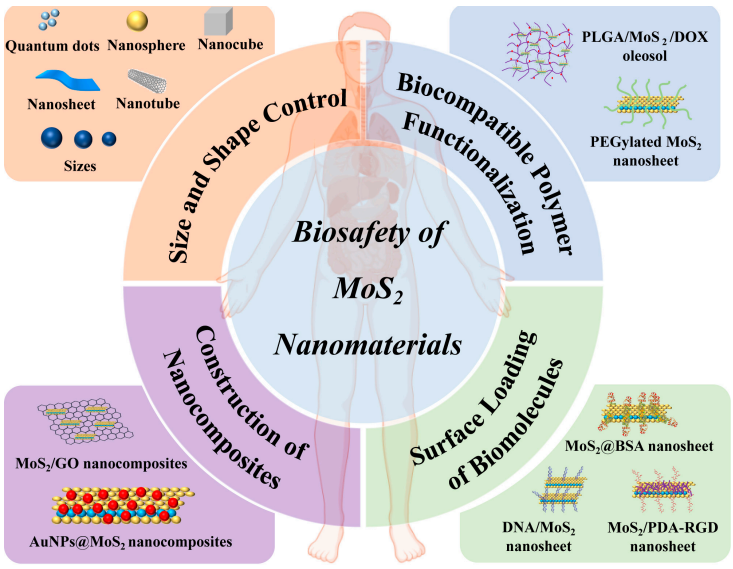

Figure 11. Illustration of the biocompatibility regulation methods for MoS_2 nanomaterials.

5. Conclusions and Perspectives

In this review, we present a comprehensive overview of the recent works on the nano–bio interaction between MoS_2 and biomolecules, as well as relevant bio-applications

and biosecurity. By combining experimental and theoretical approaches, a comprehensive understanding of the intricate interactions between MoS_2 and key biomolecules, including amino acids, peptides, proteins, DNA, and biological membranes, has been summarized. These nano–bio interfacial interactions include hydrophobic interactions, electrostatic interactions, van der Waals forces and π–π stacking interactions between biomolecules and nanomaterials. Additionally, it is directly determined by the biomolecule's composition, three-dimensional conformation and position relative to the nanomaterial of these biomolecules. In particular, based on these specific nano–bio interactions, the development of related application fields can be promoted, such as peptide detection, DNA sequencing, etc. In addition, the morphology, size, surface physical, and chemical properties of MoS_2 nanomaterials are directly related to their biological safety. Therefore, it has emerged as a prominent area of the research field to modify the surface structure through biomolecule interaction to reduce biotoxicity and promote in vivo medical and biological applications.

However, there are still some issues and challenges to be settled. Firstly, the biosafety issue arising from the ingestion of nanomaterials into organisms is a matter of significant concern. Once nanomaterials enter the systemic circulation, they inevitably engage in interactions with numerous biomolecules through the nano–bio interfacial interactions, resulting in the formation of coronal complexes commonly referred to as "protein corona". Importantly, it would further modulate the physiochemical properties and pharmacological behavior of nanomaterials in vivo, including targeting ability, circulation kinetics, clearance mechanisms, and immune response. In fact, it is complex and non-intuitive to evaluate the long-term toxicological effects of MoS_2-based nanomaterials due to the inherent complexity of biological systems. To address this, considerable efforts are required to understand the unique nano–bio interfacial interactions and unravel the cellular and subcellular responses of biological molecules upon the introduction of MoS_2. While many studies have contributed to our understanding of the interaction between MoS_2 and biomolecules, the comprehensive exploration of the biosafety of nanomaterials through in vitro, in vivo, and organic studies remains necessary. Moreover, exploring potential biomedical applications based on the various nano–bio interactions can yield valuable insights for the development of new materials with specific targeting capabilities, thereby accelerating the advancement of MoS_2-based biomedical materials. Such endeavors are essential to ensuring responsible and rapid applications in clinical and biomedical domains of MoS_2, as well as other nanomaterials.

Author Contributions: Conceptualization, writing—original draft, R.W.; review and editing, R.W., L.L. and M.D. All authors have read and agreed to the published version of the manuscript.

Funding: This work was supported by the National Natural Science Foundation of China (NO. 22072060).

Institutional Review Board Statement: Not applicable.

Informed Consent Statement: Not applicable.

Data Availability Statement: The data presented in this study are available on request from the corresponding author.

Conflicts of Interest: The authors declare no conflict of interest.

References

1. Tan, L.F.; Wang, S.P.; Xu, K.; Liu, T.L.; Liang, P.; Niu, M.; Fu, C.H.; Shao, H.B.; Yu, J.; Ma, T.C.; et al. Layered MoS_2 hollow spheres for highly-efficient photothermal therapy of rabbit liver orthotopic transplantation tumors. *Small* **2016**, *12*, 2046–2055. [CrossRef] [PubMed]
2. Li, F.; Hu, S.H.; Zhang, R.; Gu, Y.J.; Li, Y.G.; Jia, Y.F. Porous graphene oxide enhanced aptamer specific circulating-tumor-cell sensing interface on light addressable potentiometric sensor: Clinical application and simulation. *ACS Appl. Mater. Interfaces* **2019**, *11*, 8704–8709. [CrossRef] [PubMed]
3. Amrollahi-Sharifabadi, M.; Koohi, M.K.; Zayerzadeh, E.; Hablolvarid, M.H.; Hassan, J.; Seifalian, A.M. In vivo toxico-logical evaluation of graphene oxide nanoplatelets for clinical application. *Int. J. Nanomed.* **2018**, *13*, 4757. [CrossRef]

4. Rao, C.N.R.; Ramakrishna Matte, H.S.S.; Maitra, U. Graphene analogues of inorganic layered materials. *Angew. Chem. Int. Ed.* **2013**, *52*, 13162–13185. [CrossRef] [PubMed]
5. Wang, H.M.; Li, C.H.; Fang, P.F.; Zhang, Z.L.; Zhang, J.Z. Synthesis, properties, and optoelectronic applications of two-dimensional MoS_2 and MoS_2-based heterostructures. *Chem. Soc. Rev.* **2018**, *47*, 6101–6127. [CrossRef]
6. Benavente, E.; Santa Ana, M.A.; Mendizabal, F.; Gonzalez, G. Intercalation chemistry of molybdenum disulfide. *Coord. Chem. Rev.* **2002**, *224*, 87–109. [CrossRef]
7. Enyashin, A.N.; Yadgarov, L.; Houben, L.; Popov, I.; Weidenbach, M.; Tenne, R.; Bar-Sadan, M.; Seifert, G. New route for stabilization of 1T-WS_2 and MoS_2 phases. *J. Phys. Chem. C* **2011**, *115*, 24586–24591. [CrossRef]
8. Chai, Y.; Su, S.S.; Yan, D.; Ozkan, M.; Lake, R.; Ozkan, C.S. Strain gated bilayer molybdenum disulfide field effect transistor with edge contacts. *Sci. Rep.* **2017**, *7*, 41593. [CrossRef]
9. Jiang, Z.Z.; Zhou, W.D.; Hong, A.J.; Guo, M.M.; Luo, X.F.; Yuan, C.L. MoS_2 moire superlattice for hydrogen evolution reaction. *ACS Energy Lett.* **2019**, *4*, 2830–2835. [CrossRef]
10. Wang, L.W.; Zhang, X.D.; You, Z.; Yang, Z.W.; Guo, M.Y.; Guo, J.W.; Liu, H.; Zhang, X.Y.; Wang, Z.; Wang, A.Z.; et al. A molybdenum disulfide nanozyme with charge-enhanced activity for ultrasound-mediated cascade-catalytic tumor ferroptosis. *Angew. Chem. Int. Ed.* **2023**, *62*, e202217448. [CrossRef]
11. Zhu, C.F.; Zeng, Z.Y.; Li, H.; Li, F.; Fan, C.H.; Zhang, H. Single-layer MoS_2-based nanoprobes for homogeneous detection of biomolecules. *J. Am. Chem. Soc.* **2013**, *135*, 5998–6001. [CrossRef]
12. Yin, W.Y.; Yan, L.; Yu, J.; Tian, G.; Zhou, L.J.; Zheng, X.P.; Zhang, X.; Yong, Y.; Li, J.; Gu, Z.J.; et al. High-throughput synthesis of single-layer MoS_2 nanosheets as a near-infrared photothermal-triggered drug delivery for effective cancer therapy. *ACS Nano* **2014**, *8*, 6922–6933. [CrossRef]
13. Liu, T.; Wang, C.; Gu, X.; Gong, H.; Cheng, L.; Shi, X.Z.; Feng, L.Z.; Sun, B.Q.; Liu, Z. Drug delivery with PEGylated MoS_2 nano-sheets for combined photothermal and chemotherapy of cancer. *Adv. Mater.* **2014**, *26*, 3433–3440. [CrossRef]
14. Liu, T.; Shi, S.X.; Liang, C.; Shen, S.; Cheng, L.; Wang, C.; Song, X.J.; Goel, S.; Barnhart, T.E.; Cai, W.B.; et al. Iron oxide deco-rated MoS_2 nanosheets with double PEGylation for chelator-free radiolabeling and multimodal imaging guided photo-thermal therapy. *ACS Nano* **2015**, *9*, 950–960. [CrossRef]
15. Zhang, X.Y.; Wu, J.R.; Williams, G.R.; Niu, S.W.; Qian, Q.Q.; Zhu, L.M. Functionalized MoS_2-nanosheets for targeted drug delivery and chemo-photothermal therapy. *Colloids Surf. B* **2019**, *173*, 101–108. [CrossRef]
16. Wu, N.; Yu, Y.D.; Li, T.; Ji, X.J.; Jiang, L.; Zong, J.J.; Huang, H. Investigating the influence of MoS_2 nanosheets on E. coli from metabolomics level. *PLoS ONE* **2016**, *11*, e0167245. [CrossRef]
17. Zhou, R.H.; Gao, H.J. Cytotoxicity of graphene: Recent advances and future perspective. *WIREs Nanomed. Nanobiotechnol.* **2014**, *6*, 452–474. [CrossRef] [PubMed]
18. Liu, T.; Liu, Z. 2D MoS_2 nanostructures for biomedical applications. *Adv. Healthcare Mater.* **2018**, *7*, 1701158. [CrossRef] [PubMed]
19. Cao, M.J.; Cai, R.; Zhao, L.N.; Guo, M.Y.; Wang, L.M.; Wang, Y.C.; Liu, Y.; Zhao, Y.L.; Chen, C.Y. Molybdenum derived from nanomaterials incorporates into molybdenum enzymes and affects their activities in vivo. *Nat. Nanotechnol.* **2021**, *16*, 708–716. [CrossRef]
20. Li, J.L.; Chen, C.Y.; Xia, T. Understanding nanomaterial–liver interactions to facilitate the development of safer nanoapplications. *Adv. Mater.* **2022**, *34*, 2106456. [CrossRef] [PubMed]
21. Baimanov, D.; Wu, J.G.; Chu, R.X.; Cai, R.; Wang, B.; Cao, M.J.; Tao, Y.; Liu, J.M.; Feng, W.Y.; Wang, L.M.; et al. Immunological responses induced by blood protein coronas on two-dimensional MoS_2 nanosheets. *ACS Nano* **2020**, *14*, 5529–5542. [CrossRef]
22. Shah, P.; Narayanan, T.N.; Li, C.Z.; Alwarappan, S. Probing the biocompatibility of MoS_2 nanosheets by cytotoxicity assay and electrical impedance spectroscopy. *Nanotechnology* **2015**, *26*, 315102. [CrossRef]
23. Moore, C.; Movia, D.; Smith, R.J.; Hanlon, D.; Lebre, F.; Lavelle, E.C.; Byrne, H.J.; Coleman, J.N.; Volkov, Y.; McIntyre, J. Industrial grade 2D molybdenum disulphide (MoS_2): An in vitro exploration of the impact on cellular uptake, cytotoxicity, and inflammation. *2D Mater.* **2017**, *4*, 025065. [CrossRef]
24. Appel, J.H.; Li, D.O.; Podlevsky, J.D.; Debnath, A.; Green, A.A.; Wang, Q.H.; Chae, J. Low cytotoxicity and genotoxicity of two-dimensional MoS_2 and WS_2. *ACS Biomater. Sci. Eng.* **2016**, *2*, 361–367. [CrossRef]
25. Ozboyaci, M.; Kokh, D.B.; Corni, S.; Wade, R.C. Modeling and simulation of protein-surface interactions: Achievements and challenges. *Q. Rev. Biophys.* **2016**, *49*, e4. [CrossRef]
26. Heinz, H.; Ramezani-Dakhel, H. Simulations of inorganic-bioorganic interfaces to discover new materials: Insights, compar-isons to experiment, challenges, and opportunities. *Chem. Soc. Rev.* **2016**, *45*, 412–448. [CrossRef]
27. Mukhopadhyay, S.; Scheicher, R.H.; Pandey, R.; Karna, S.P. Sensitivity of boron nitride nanotubes toward biomolecules of different polarities. *J. Phys. Chem. Lett.* **2016**, *2*, 2442–2447. [CrossRef]
28. Isidro-Llobet, A.; Alvarez, M.; Albericio, F. Amino acid-protecting groups. *Chem. Rev.* **2009**, *109*, 2455–2504. [CrossRef]
29. Zhang, P.; Wang, Z.G.; Liu, L.; Klausen, L.H.; Wang, Y.; Mi, J.L.; Dong, M.D. Modulation the electronic property of 2D monolayer MoS_2 by amino acid. *Appl. Mater. Today* **2019**, *14*, 151–158. [CrossRef]
30. Huyen, T.L.; Lee, C.H.; Cheng, S.J.; Yang, C.K. Interaction between peptides and an MoS_2 monolayer containing a nanopore: First-principles calculations. *Chin. J. Phys.* **2022**, *1*, 1. [CrossRef]
31. Dalle-Donne, I.; Giustarini, D.; Colombo, R.; Rossi, R.; Milzani, A. Protein carbonylation in human diseases. *Trends Mol. Med.* **2003**, *9*, 169–176. [CrossRef]

32. Kapurniotu, A. Enlightening amyloid fibrils linked to type 2 diabetes and cross-interactions with Aβ. *Nat. Struct. Mol. Biol.* **2020**, *27*, 1006–1008. [CrossRef]
33. Wu, R.R.; Ou, X.W.; Zhang, L.W.; Song, X.L.; Wang, Z.K.; Dong, M.D.; Liu, L. Electric field effect on inhibiting the co-fibrillation of amyloid peptides by modulating the aggregation pathway. *Langmuir* **2022**, *38*, 12346–12355. [CrossRef] [PubMed]
34. Bu, X.L.; Xiang, Y.; Jin, W.S.; Wang, J.; Shen, L.L.; Huang, Z.L.; Zhou, H.D.; Zhou, X.F.; Song, W.; Wang, Y.J. Blood-derived amyloid-β protein induces Alzheimer's disease pathologies. *Mol. Psychiatry* **2018**, *23*, 1948–1956. [CrossRef] [PubMed]
35. Wu, R.R.; Ou, X.W.; Zhang, L.W.; Wang, F.H.; Liu, L. Interfacial interactions within amyloid protein corona based on 2D MoS_2 nanosheets. *ChemBioChem* **2022**, *23*, e202100581. [CrossRef]
36. Xiao, M.Y.; Wei, S.; Li, Y.X.; Jasensky, J.; Chen, J.; Brooks, C.L.; Chen, Z. Molecular interactions between single layered MoS_2 and biological molecules. *Chem. Sci.* **2018**, *9*, 1769–1773. [CrossRef] [PubMed]
37. Ling, Y.; Gu, Z.L.; Kang, S.G.; Luo, J.D.; Zhou, R.H. Structural damage of a β-sheet protein upon adsorption onto molybdenum disulfide nanotubes. *J. Phys. Chem. C.* **2016**, *120*, 6796–6803. [CrossRef]
38. Hsu, H.J.; Sheu, S.Y.; Tsay, R.Y. Preferred orientation of albumin adsorption on a hydrophilic surface from molecular simulation. *Colloids Surf. B* **2008**, *67*, 183–191. [CrossRef]
39. Xiao, M.Y.; Wei, S.; Chen, J.J.; Tian, J.Y.; Brooks Iii, C.L.; Marsh, E.N.G.; Chen, Z. Molecular mechanisms of interactions between monolayered transition metal dichalcogenides and biological molecules. *J. Am. Chem. Soc.* **2019**, *141*, 9980–9988. [CrossRef]
40. Chen, X.; Berner, N.C.; Backes, C.; Duesberg, G.S.; McDonald, A.R. Functionalization of two-dimensional MoS_2: On the reaction between MoS_2 andorganic thiols. *Angew. Chem. Int. Ed.* **2016**, *55*, 5803–5808. [CrossRef]
41. Fan, H.J.; Zhao, D.H.; Li, Y.T.; Zhou, J. Lysozyme orientation and conformation on MoS_2 surface: Insights from molecular sim-ulations. *Biointerphases* **2017**, *12*, 416. [CrossRef]
42. Mudedla, S.K.; Murugan, N.A.; Subramanian, V.; Agren, H. Destabilization of amyloid fibrils on interaction with MoS_2-based nanomaterials. *RSC Adv.* **2019**, *9*, 1613–1624. [CrossRef]
43. Gu, Z.L.; Plant, L.D.; Meng, X.Y.; Perez-Aguilar, J.M.; Wang, Z.; Dong, M.D.; Logothetis, D.E.; Zhou, R.H. Exploring the nano-toxicology of MoS_2: A study on the interaction of MoS_2 nanoflakes and K^+ channels. *ACS Nano* **2018**, *12*, 705–717. [CrossRef]
44. Gu, Z.L.; Song, W.; Liu, S.T.; Li, B.Y.; Plant, L.D.; Meng, X.Y. Potential blockade of the human voltage-dependent anion channel by MoS_2 nanoflakes. *Phys. Chem. Chem. Phys.* **2019**, *21*, 9520–9530. [CrossRef] [PubMed]
45. Yang, X.; Li, J.; Liang, T.; Ma, C.Y.; Zhang, Y.Y.; Chen, H.Z.; Hanagata, N.; Su, H.X.; Xu, M.S. Antibacterial activity of two-dimensional MoS_2 sheets. *Nanoscale* **2014**, *6*, 10126–10133. [CrossRef] [PubMed]
46. Hirano, A.; Uda, K.; Maeda, Y.; Akasaka, T.; Shiraki, K. One-dimensional protein-based nanoparticles induce lipid bilayer disruption: Carbon nanotube conjugates and amyloid fibrils. *Langmuir* **2010**, *26*, 17256–17259. [CrossRef]
47. Gilbertson, L.M.; Albalghiti, E.M.; Fishman, Z.S.; Perreault, F.O.; Corredor, C.; Posner, J.D.; Elimelech, M.; Pfefferle, L.D.; Zimmerman, J.B. Shape-dependent surface reactivity and antimicrobial activity of nano-cupric oxide. *Environ. Sci. Technol.* **2016**, *50*, 3975–3984. [CrossRef] [PubMed]
48. Moghadam, B.Y.; Hou, W.C.; Corredor, C.; Westerhoff, P.; Posner, J.D. Role of nanoparticle surface functionality in the disruption of model cell membranes. *Langmuir* **2012**, *28*, 16318–16326. [CrossRef]
49. Zucker, I.; Werber, J.R.; Fishman, Z.S.; Hashmi, S.M.; Gabinet, U.R.; Lu, X.L.; Osuji, C.O.; Pfefferle, L.D.; Elimelech, M. Loss of phospholipid membrane integrity induced by two-dimensional nanomaterials. *Environ. Sci. Technol. Lett.* **2017**, *4*, 404–409. [CrossRef]
50. Tu, Y.S.; Lv, M.; Xiu, P.; Huynh, T.; Zhang, M.; Castelli, M.; Liu, Z.R.; Fan, C.H.; Fang, H.P.; Zhou, R.H. Destructive extraction of phospholipids from Esche-richia coli membranes by graphene nanosheets. *Nat. Nanotechnol.* **2013**, *8*, 594–601. [CrossRef]
51. Wu, R.R.; Ou, X.W.; Tian, R.R.; Zhang, J.; Jin, H.S.; Dong, M.D.; Li, J.Y.; Liu, L. Membrane destruction and phospholipid extraction by using two-dimensional MoS_2 nanosheets. *Nanoscale* **2018**, *10*, 20162–20170. [CrossRef]
52. Zhou, X.F.; Jia, J.B.; Luo, Z.; Su, G.X.; Yue, T.T.; Yan, B. Remote induction of cell autophagy by 2D MoS_2 nanosheets via per-turbing cell surface receptors and mTOR pathway from outside of cells. *ACS Appl. Mater. Interfaces* **2019**, *11*, 6829–6839. [CrossRef]
53. Zhang, W.; Chen, Y.Z.; Huynh, T.; Yang, Y.Q.; Yang, X.Q.; Zhou, R.H. Directional extraction and penetration of phosphorene nanosheets to cell membranes. *Nanoscale* **2020**, *12*, 2810–2819. [CrossRef] [PubMed]
54. Garaj, S.; Hubbard, W.; Reina, A.; Kong, J.; Branton, D.; Golovchenko, J.A. Graphene as a subnanometre trans-electrode membrane. *Nature* **2010**, *467*, 190–193. [CrossRef]
55. Lv, W.; Liu, S.; Li, X.; Wu, R.A. Spatial blockage of ionic current for electrophoretic translocation of DNA through a graphene nanopore. *Electrophoresis* **2014**, *35*, 1144–1151. [CrossRef]
56. Qiu, H.; Sarathy, A.; Leburton, J.; Schulten, K. Intrinsic stepwise translocation of stretched ssDNA in graphene nanopores. *Nano Lett.* **2015**, *15*, 8322–8330. [CrossRef] [PubMed]
57. Qiu, H.; Sarathy, A.; Schulten, K.; Leburton, J.P. Detection and mapping of DNA methylation with 2D material nanopores. *Npj 2D Mater. Appl.* **2017**, *1*, 3. [CrossRef]
58. Luan, B.Q.; Zhou, R.H. Spontaneous transport of single-stranded DNA through graphene-MoS_2 heterostructure nanopores. *ACS Nano* **2018**, *12*, 3886–3891. [CrossRef]
59. Kiriya, D.; Tosun, M.; Zhao, P.D.; Kang, J.S.; Javey, A. Air-stable surface charge transfer doping of MoS_2 by benzyl vi-ologen. *J. Am. Chem. Soc.* **2014**, *136*, 7853–7856. [CrossRef] [PubMed]

60. Sarkar, D.; Liu, W.; Xie, X.; Anselmo, A.C.; Mitragotri, S.; Banerjee, K. MoS_2 field-effect transistor for next-generation label-free biosensors. *ACS Nano* **2014**, *8*, 3992–4003. [CrossRef]
61. Reiner, J.E.; Balijepalli, A.; Robertson, J.W.F.; Campbell, J.; Suehle, J.; Kasianowicz, J.J. Disease detection and manage-ment via single nanopore-based sensors. *Chem. Rev.* **2012**, *112*, 6431–6451. [CrossRef] [PubMed]
62. Freedman, K.J.; Bastian, A.R.; Chaiken, I.; Kim, M.J. Solid-state nanopore detection of protein complexes: Applications in healthcare and protein kinetics. *Small* **2013**, *9*, 750–759. [CrossRef] [PubMed]
63. Noguchi, H.; Nakamura, Y.; Tezuka, S.; Seki, T.; Yatsu, K.; Narimatsu, T.; Nakata, Y.; Hayamizu, Y.H. Self-assembled GA-repeated peptides as a biomolecular scaffold for biosensing with MoS_2 electrochemical transistors. *ACS Appl. Mater. Interfaces* **2023**, *15*, 14058–14066. [CrossRef]
64. Si, W.; Yuan, R.Y.; Wu, G.S.; Kan, Y.J.; Sha, J.J.; Chen, Y.F.; Zhang, Y.; Shen, Y. Navigated delivery of peptide to the nanopore using in-plane heterostructures of MoS_2 and SnS_2 for protein sequencing. *J. Phys. Chem. Lett.* **2022**, *13*, 3863–3872. [CrossRef] [PubMed]
65. Gu, L.Q.; Shim, J.W. Single molecule sensing by nanopores and nanopore devices. *Analyst* **2010**, *135*, 441–451. [CrossRef] [PubMed]
66. Rosen, C.B.; Rodriguez-Larrea, D.; Bayley, H. Single-molecule site-specific detection of protein phosphorylation with a nanopore. *Nat. Biotechnol.* **2014**, *32*, 179–181. [CrossRef]
67. Kukkar, M.; Sharma, A.; Kumar, P.; Kim, K.H.; Deep, A. Application of MoS_2 modified screen-printed electrodes for highly sensitive detection of bovine serum albumin. *Anal. Chim. Acta* **2016**, *939*, 101–107. [CrossRef]
68. Gogoi, S.; Khan, R. Fluorescence immunosensor for cardiac troponin T based on forster resonance energy transfer (FRET) between carbon dot and MoS_2 nano-couple. *Phys. Chem. Chem. Phys.* **2018**, *20*, 16501–16509. [CrossRef]
69. Lee, J.; Dak, P.; Lee, Y.; Park, H.; Choi, W.; Alam, M.A.; Kim, S. Two-dimensional layered MoS_2 biosensors enable highly sensitive detection of biomolecules. *Sci. Rep.* **2014**, *4*, 7352. [CrossRef]
70. Sajid, M.; Osman, A.; Siddiqui, G.U.; Kim, H.B.; Kim, S.W.; Ko, J.B.; Choi, K.H. All-printed highly sensitive 2D MoS_2 based multi-reagent immunosensor for smartphone based point-of-care diagnosis. *Sci. Rep.* **2017**, *7*, 5802. [CrossRef]
71. Giordano, B.C.; Ferrance, J.; Swedberg, S.; Huhmer, A.F.R.; Landers, J.P. Polymerase chain reaction in polymeric micro-chips: DNA amplification in less than 240 seconds. *Anal. Biochem.* **2001**, *291*, 124–132. [CrossRef]
72. Zhang, Y.; Zheng, B.; Zhu, C.F.; Zhang, X.; Tan, C.L.; Li, H.; Chen, B.; Yang, J.; Chen, J.Z.; Huang, Y.; et al. Single-layer transi-tion metal dichalcogenide nanosheet-based nanosensors for rapid, sensitive, and multiplexed detection of DNA. *Adv. Mater.* **2015**, *27*, 935–939. [CrossRef]
73. Zhang, W.; Dai, Z.C.; Liu, X.; Yang, J.M. High-performance electrochemical sensing of circulating tumor DNA in peripheral blood based on poly-xanthurenic acid functionalized MoS_2 nanosheets. *Biosens. Bioelectron.* **2018**, *105*, 116–120. [CrossRef]
74. Wang, T.Y.; Zhu, R.Z.; Zhuo, J.Q.; Zhu, Z.W.; Shao, Y.H.; Li, M.X. Direct detection of DNA below ppb level based on thio-nin-functionalized layered MoS_2 electrochemical sensors. *Anal. Chem.* **2014**, *86*, 12064–12069. [CrossRef]
75. Li, F.; Cui, X.T.; Zheng, Y.L.; Wang, Q.; Zhou, Y.L.; Yin, H.S. Photoelectrochemical biosensor for DNA formylation based on WS_2 nanosheets@polydopamine and MoS_2 nanosheets. *Biosens. Bioelectron. X* **2022**, *10*, 100104. [CrossRef]
76. Oudeng, G.; Au, M.T.; Shi, J.Y.; Wen, C.Y.; Yang, M. One-step in situ detection of miRNA-21 expression in single cancer cells based on biofunctionalized MoS_2 nanosheets. *ACS Appl. Mater. Interfaces* **2018**, *10*, 350–360. [CrossRef]
77. Wasfi, A.; Awwad, F.; Atef, M. DNA bases detection via MoS_2 field effect transistor with a nanopore: First-principles modeling. *Analog Integr. Circuits Signal Process.* **2023**, *114*, 253–264. [CrossRef]
78. Xiao, M.S.; Chandrasekaran, A.R.; Ji, W.; Li, F.; Man, T.T.; Zhu, C.F.; Shen, X.Z.; Pei, H.; Li, Q.; Li, L. Affinity-modulated molec-ular beacons on MoS_2 nanosheets for microRNA detection. *ACS Appl. Mater. Interfaces* **2018**, *10*, 35794–35800. [CrossRef] [PubMed]
79. Liu, K.; Feng, J.D.; Kis, A.; Radenovic, A. Atomically thin molybdenum disulfide nanopores with high sensitivity for DNA translocation. *ACS Nano* **2014**, *8*, 2504–2511. [CrossRef]
80. Chakraborty, R.; Xiong, M.Y.; Athreya, N.; Tabatabaei, S.K.; Milenkovic, O.; Leburton, J.P. Solid-state MoS_2 nanopore membranes for discriminating among the lengths of RNA tails on a double-stranded DNA: A new simulation-based differentiating algorithm. *ACS Appl. Nano Mater.* **2023**, *6*, 4651–4660. [CrossRef]
81. Gu, C.M.; Yu, Z.B.; Li, X.J.; Zhu, X.; Jin, C.H.; Cao, Z.; Dong, S.R.; Luo, J.K.; Ye, Z.; Liu, Y. Experimental study on single biomolecule sensing using MoS_2–graphene heterostructure nanopores. *Nanoscale* **2023**, *15*, 266–272. [CrossRef]
82. Roy, S.; Mondal, A.; Yadav, V.; Sarkar, A.; Banerjee, R.; Sanpui, P.; Jaiswal, A. Mechanistic insight into the antibacterial activity of chitosan exfoliated MoS_2 nanosheets: Membrane damage, meta-bolic inactivation, and oxidative stress. *ACS Appl. Bio Mater.* **2019**, *2*, 2738–2755. [CrossRef]
83. Yin, W.Y.; Yu, J.; Lv, F.T.; Yan, L.; Zheng, L.R.; Gu, Z.J.; Zhao, Y. Functionalized anano-MoS_2 with peroxidase catalytic and near-infrared photothermal activities for safe and synergetic wound antibacterial applications. *ACS Nano* **2016**, *10*, 11000–11011. [CrossRef] [PubMed]
84. Gao, Q.; Zhang, X.; Yin, W.Y.; Ma, D.Q.; Xie, C.J.; Zheng, L.R.; Dong, X.H.; Mei, L.Q.; Yu, J.; Wang, C.Z.; et al. Functionalized MoS_2 nanovehicle with near-infrared laser-mediated nitric oxide release and photothermal activities for advanced bacteria-Infected wound therapy. *Small* **2018**, *14*, 1802290. [CrossRef] [PubMed]
85. Roy, S.; Haloi, P.; Choudhary, R.; Chawla, S.; Kumari, M.; Konkimalla, V.B.; Jaiswal, A. Quaternary pullulan-functionalized 2D MoS_2 glycosheets: A potent bactericidal nanoplatform for efficient wound disinfection and healing. *ACS Appl. Mater. Interfaces* **2023**, *15*, 24209–24227. [CrossRef]

86. Teo, W.Z.; Chng, E.L.K.; Sofer, Z.; Pumera, M. Cytotoxicity of exfoliated transition-metal dichalcogenides (MoS_2, WS_2, and WSe_2) is lower than that of graphene and its analogues. *Chem. Eur. J.* **2014**, *20*, 9627–9632. [CrossRef] [PubMed]
87. Fan, J.J.; Li, Y.F.; Nguyen, H.N.; Yao, Y.; Rodrigues, D.F. Toxicity of exfoliated-MoS_2 and annealed exfoliated-MoS_2 to-wards planktonic cells, biofilms, and mammalian cells in the presence of electron donor. *Environ. Sci.-Nano* **2015**, *2*, 370–379. [CrossRef]
88. Chng, E.L.K.; Sofer, Z.; Pumera, M. MoS_2 exhibits stronger toxicity with increased exfoliation. *Nanoscale* **2014**, *6*, 14412–14418. [CrossRef] [PubMed]
89. Wu, H.H.; Yang, R.; Song, B.M.; Han, Q.S.; Li, J.Y.; Zhang, Y.; Fang, Y.; Tenne, R.; Wang, C. Biocompatible inorganic fullerene-like molybdenum disulfide nanoparticles produced by pulsed laser ablation in water. *ACS Nano* **2011**, *5*, 1276–1281. [CrossRef]
90. Wu, B.; Chen, L.; Wu, X.M.; Hou, H.; Wang, Z.Z.; Liu, S. Differential influence of molybdenum disulfide at the nanometer and micron scales in the intestinal metabolome and mi-crobiome of mice. *Environ. Sci. Nano* **2019**, *6*, 1594–1606. [CrossRef]
91. Hao, J.L.; Song, G.S.; Liu, T.; Yi, X.; Yang, K.; Cheng, L.; Liu, Z. In vivo long-term biodistribution, excretion, and toxicology of PEGylated transition-metal dichalcogenides MS_2 (M = Mo, W, Ti) nanosheets. *Adv. Sci.* **2017**, *4*, 1600160. [CrossRef]
92. Wang, S.G.; Li, K.; Chen, Y.; Chen, H.R.; Ma, M.; Feng, J.W.; Zhao, Q.H.; Shi, J.L. Biocompatible PEGylated MoS_2 nanosheets: Controllable bottom-up synthesis and highly efficient photothermal regression of tumor. *Biomaterials* **2015**, *39*, 206–217. [CrossRef] [PubMed]
93. Wang, S.G.; Chen, Y.; Li, X.; Gao, W.; Zhang, L.L.; Liu, J.; Zheng, Y.Y.; Chen, H.R.; Shi, J.L. Injectable 2D MoS_2-integrated drug delivering implant for highly efficient NIR-triggered synergistic tumor hyperthermia. *Adv. Mater.* **2015**, *27*, 7117–7122. [CrossRef]
94. Chen, L.; Feng, Y.H.; Zhou, X.J.; Zhang, Q.Q.; Nie, W.; Wang, W.Z.; Zhang, Y.Z.; He, C.L. One-pot synthesis of MoS_2 nanoflakes with desirable degradability for photothermal cancer therapy. *ACS Appl. Mater. Interfaces* **2017**, *9*, 17347–17358. [CrossRef]
95. Chen, L.; Feng, W.; Zhou, X.J.; Qiu, K.X.; Miao, Y.K.; Zhang, Q.Q.; Qin, M.; Li, L.; Zhang, Y.Z.; He, C.L. Facile synthesis of novel albumin-functionalized flower-like MoS_2 nanoparticles for in vitro chemo-photothermal synergistic therapy. *RSC Adv.* **2016**, *6*, 13040–13049. [CrossRef]
96. Pang, B.; Yang, H.R.; Wang, L.Y.; Chen, J.Q.; Jin, L.H.; Shen, B.J. Aptamer modified MoS_2 nanosheets application in targeted photothermal therapy for breast cancer. *Colloids Surf. A* **2021**, *608*, 125506. [CrossRef]
97. Wu, J.R.; Bremner, D.H.; Niu, S.W.; Wu, H.L.; Wu, J.Z.; Wang, H.J.; Li, H.Y.; Zhu, L.M. Functionalized MoS_2 nanosheet-capped periodic mesoporous organosilicas as a multifunctional platform for synergistic targeted chemo-photothermal therapy. *Chem. Eng. J* **2018**, *342*, 90–102. [CrossRef]
98. Li, B.L.; Setyawati, M.I.; Chen, L.Y.; Xie, J.P.; Ariga, K.; Lim, C.T.; Garaj, S.; Leong, D.T. Directing assembly and disassembly of 2D MoS_2 nanosheets with DNA for drug delivery. *ACS Appl. Mater. Interfaces* **2017**, *9*, 15286–15296. [CrossRef]
99. Song, I.; Park, C.; Choi, H.C. Synthesis and properties of molybdenum disulphide: From bulk to atomic layers. *RSC Adv.* **2015**, *5*, 7495–7514. [CrossRef]
100. Yuan, Z.; Tao, B.L.; He, Y.; Liu, J.; Lin, C.C.; Shen, X.K.; Ding, Y.; Yu, Y.L.; Mu, C.Y.; Liu, P.; et al. Biocompatible MoS_2/PDA-RGD coating on titanium implant with antibacterial property via intrinsic ROS-independent oxidative stress and NIR irradiation. *Biomaterials* **2019**, *217*, 119290. [CrossRef] [PubMed]
101. Kumar, R.; Bunekar, N.; Dutt, S.; Reddy, P.G.; Gupta, A.K.; Aadil, K.R.; Mishra, V.K.; Singh, S.; Sarkar, C. 2D advanced functional nanomaterials for cancer therapy. *2D Funct. Nanomater.* **2021**, *1*, 199–233.